

Quantum stabilizer codes for correlated and asymmetric depolarizing errors

Carlo Cafaro and Stefano Mancini

School of Science and Technology, Physics Division, University of Camerino, I-62032 Camerino, Italy

(Received 13 May 2010; published 9 July 2010)

We study the performance of common quantum stabilizer codes in the presence of asymmetric and correlated errors. Specifically, we consider the depolarizing noisy quantum memory channel and perform quantum error correction via the five- and seven-qubit stabilizer codes. We characterize these codes by means of the entanglement fidelity as a function of the error probability and the degree of memory. We show that their performances are lowered by the presence of correlations, and we compute the error probability threshold values for code effectiveness. Furthermore, we uncover that the asymmetry in the error probabilities does not affect the performance of the five-qubit code, while it does affect the performance of the seven-qubit code, which results in being less effective when considering correlated and symmetric depolarizing errors but more effective for correlated and asymmetric errors.

DOI: [10.1103/PhysRevA.82.012306](https://doi.org/10.1103/PhysRevA.82.012306)

PACS number(s): 03.67.Pp

I. INTRODUCTION

The most important obstacle in quantum information processing is decoherence. It causes a quantum computer to lose its quantum properties, destroying its performance advantages over a classical computer. The unavoidable interaction between the open quantum processor and its environment corrupts the information stored in the system and causes errors that may lead to wrong outputs. In general, environments may be very complex systems characterized by many uncontrollable degrees of freedom. A useful active strategy to defend quantum coherence of processing against environmental noise is that of quantum-error-correcting codes (QECCs) [1–3], where, in analogy to classical information theory, quantum information is stabilized using redundant encoding and measurements.

The formal mathematical description of the qubit-environment interaction is often given in terms of quantum channels. Quantum error correction (QEC) is usually developed under the assumption of identically and independently distributed errors. These error models are characterized by memoryless communication channels Λ such that n -channel uses is given by $\Lambda^{(n)} = \Lambda^{\otimes n}$. In such cases of completely independent decoherence, qubits interact with their own environments, which do not interact with each other. However, in actual physical situations, qubits may interact with a common environment, which unavoidably introduces correlations in the noise. For instance, there are situations where qubits in an ion trap setup are collectively coupled to their vibrational modes [4]. In other situations, different qubits in a quantum dot design are coupled to the same lattice, thus interacting with a common thermal bath of phonons [5]. The exchange of bosons between qubits causes spatial and temporal correlations that violate the condition of error independence [6]. Memory effects introduce correlations among channel uses with the consequence that $\Lambda^{(n)} \neq \Lambda^{\otimes n}$. Recent studies have tried to characterize the effect of correlations on the performance of QECCs [7–11]. It appears that correlations may have negative [8] or positive [9] impacts on QECCs, depending on the features of the error model being considered.

Furthermore, the noise may be asymmetric. Most of the quantum computing devices [12] are characterized by relax-

ation times ($\tau_{\text{relaxation}}$) that are 1–2 orders of magnitude larger than the corresponding dephasing times ($\tau_{\text{dephasing}}$). Relaxation leads to both bit-flip and phase-flip errors, whereas dephasing (loss of phase coherence, phase shifting) only leads to phase-flip errors. Such asymmetry between $\tau_{\text{relaxation}}$ and $\tau_{\text{dephasing}}$ translates to an asymmetry in the occurrence probability of bit-flip (p_X) and phase-flip errors (p_Z). The ratio p_Z/p_X is known as the channel asymmetry. QEC schemes should be designed in such a way that no resources (time and qubits) are wasted in attempting to detect and correct errors that may be relatively unlikely to occur. Quantum codes should be designed in order to exploit this asymmetry and provide better performance by neglecting the correction of less probable errors [13–15]. Indeed, examples of efficient QECC [e.g., asymmetric stabilizer Calderbank-Shor-Steane (CSS) codes] taking advantage of this asymmetry are given by families of codes of the CSS type [16,17].

Following these lines of investigation, in this article, we study the performance of common quantum stabilizer codes in the presence of asymmetric and correlated errors. Specifically, we consider the depolarizing noisy quantum memory channel and perform QEC via the five- and seven-qubit stabilizer codes [18]. We characterize the performance of the codes by means of the entanglement fidelity $\mathcal{F}(\mu, p)$ [19] as a function of the error probability p and degree of memory μ (correlations). We show that the performance of both codes is lowered in the presence of correlations, and error probability threshold values for code effectiveness are computed versus the degree of memory μ . The error-correction schemes here considered only work for low values of μ . Furthermore, we uncover that the asymmetry in the error probabilities does not affect the performance of the five-qubit code, while it does affect the performance of the seven-qubit code, which is less effective when considering correlated and symmetric depolarizing errors but more effective for correlated and asymmetric errors.

The layout of the article is as follows. In Sec. II, we consider a depolarizing noisy quantum memory channel characterized by symmetric error probabilities, and QEC is performed via the $[[5, 1, 3]]$ stabilizer code. The performance of QECC is quantified by means of the entanglement fidelity $\mathcal{F}^{[[5, 1, 3]]}(\mu, p)$ as a function of the error probability p and degree of memory μ .

In Sec. III, QEC is performed via the $[[7,1,3]]$ -CSS stabilizer code. The performance of QECC is quantified by means of the entanglement fidelities $\mathcal{F}_{\text{Set-1}}^{[[7,1,3]]}(\mu, p)$ and $\mathcal{F}_{\text{Set-2}}^{[[7,1,3]]}(\mu, p)$ as a function of the error probability p and degree of memory μ evaluated for two different allowable sets of correctable error operators. In Sec. IV, for asymmetric error probabilities and correlated noise errors, we show that the seven-qubit code can outperform the five-qubit code and is also endowed with a better threshold curve $\mu_{\text{th}} = \mu_{\text{th}}(p)$, where error correction is performed in an effective way. Finally, in Sec. V, we present our final remarks.

II. THE FIVE-QUBIT CODE: SYMMETRIC ERROR PROBABILITIES AND CORRELATIONS

In this section, we consider a depolarizing noisy quantum memory channel with symmetric error probabilities, and QEC is performed via the $[[5,1,3]]$ stabilizer code. The performance of QECCs is quantified by means of the entanglement fidelity $\mathcal{F}^{[[5,1,3]]}(\mu, p)$ as a function of the error probability p and degree of memory μ .

A. Error model

The depolarizing channel is especially easy to analyze in the context of QEC because it has a simple interpretation in terms of the four basic errors I, X, Y, Z , which are the most commonly used in the analysis of quantum codes. However, this error model is rather general since the ability to error-correct the depolarizing channel automatically implies the ability to error-correct an arbitrary single qubit quantum operation. To simplify the notation, we may choose sometimes to omit the symbol of the tensor product, \otimes , in the expressions for the error operators of weight greater than 1.

Consider five qubits and Markov-correlated errors in a depolarizing quantum channel $\Lambda^{(5)}(\rho)$:

$$\Lambda^{(5)}(\rho) = \sum_{i_1, i_2, i_3, i_4, i_5=0}^3 p_{i_5|i_4} p_{i_4|i_3} p_{i_3|i_2} p_{i_2|i_1} p_{i_1} \times [A_{i_5} A_{i_4} A_{i_3} A_{i_2} A_{i_1} \rho A_{i_1}^\dagger A_{i_2}^\dagger A_{i_3}^\dagger A_{i_4}^\dagger A_{i_5}^\dagger], \quad (1)$$

where $A_0 \equiv I$, $A_1 \equiv X$, $A_2 \equiv Y$, $A_3 \equiv Z$ are the Pauli operators, defined as

$$\begin{aligned} I|q\rangle &:= |q\rangle, & X|q\rangle &:= |q \oplus 1\rangle, & Z|q\rangle &:= (-1)^q |q\rangle, \\ Y|q\rangle &:= i(-1)^q |q \oplus 1\rangle, \end{aligned} \quad (2)$$

with $q = 0, 1$ and X, Y and Z given by

$$\begin{aligned} X &= \begin{pmatrix} 0 & 1 \\ 1 & 0 \end{pmatrix}, & Y &= iXZ = \begin{pmatrix} 0 & -i \\ i & 0 \end{pmatrix}, \\ Z &= \begin{pmatrix} 1 & 0 \\ 0 & -1 \end{pmatrix}. \end{aligned} \quad (3)$$

The coefficients $p_{i_l|i_m}$ (conditional probabilities) with $l, m \in \{0, 1, \dots, 5\}$ satisfy the normalization condition.

$$\sum_{i_1, i_2, i_3, i_4, i_5=0}^3 p_{i_5|i_4} p_{i_4|i_3} p_{i_3|i_2} p_{i_2|i_1} p_{i_1} = 1. \quad (4)$$

For the depolarizing channel $\Lambda^{(5)}(\rho)$, coefficients $p_{i_l|i_m}$ are considered as

$$\begin{aligned} p_{k|j} &:= (1 - \mu)p_k + \mu\delta_{k,j}, & p_{k=0} &= 1 - p, \\ p_{k=1,2,3} &= p/3, \end{aligned} \quad (5)$$

where $p \in [0, 1]$ denotes the error probability, $\mu \in [0, 1]$ represents the degree of memory ($\mu = 0$ gives the uncorrelated errors and $\mu = 1$ gives perfectly correlated errors), and $p_{k|j}$ is the probability of error k on qubit j . To simplify the notation, we may choose to suppress the bar appearing in the conditional probabilities ($p_{k|j} \equiv p_{kj}$). Furthermore, since we are initially assuming $p_1 = p_2 = p_3 = p/3$, we are in the case of symmetric error probabilities.

B. Error operators

In an explicit way, the depolarizing channel $\Lambda^{(5)}(\rho)$ can be written as

$$\Lambda^{(5)}(\rho) = \sum_{k=0}^{2^{10}-1} A'_k \rho A_k^\dagger, \quad (6)$$

where A'_k are the enlarged error operators acting on the five-qubit quantum states. The cardinality of the error operators defining $\Lambda^{(5)}(\rho)$ is 2^{10} and is obtained by noticing that

$$\sum_{m=0}^5 3^m \binom{5}{m} = 2^{10}, \quad (7)$$

where $3^m \binom{5}{m}$ is the cardinality of weight- m error operators A'_k . More details on the explicit expressions for weight-0 and weight-1 appear in Appendix A.

C. Encoding

The $[[5,1,3]]$ code is the smallest single-error correcting quantum code [20]. Of all QECCs that encode one qubit of data and correct all single-qubit errors, the $[[5,1,3]]$ code is the most efficient, saturating the quantum Hamming bound. It encodes $k = 1$ qubit in $n = 5$ qubits. The cardinality of its stabilizer group \mathcal{S} is $|\mathcal{S}| = 2^{n-k} = 16$, and the set $\mathcal{B}_S^{[[5,1,3]]}$ of $n - k = 4$ group generators is given by [21]

$$\begin{aligned} \mathcal{B}_S^{[[5,1,3]]} &:= \{X^1 Z^2 Z^3 X^4, X^2 Z^3 Z^4 X^5, \\ &X^1 X^3 Z^4 Z^5, Z^1 X^2 X^4 Z^5\}. \end{aligned} \quad (8)$$

The distance of the code is $d = 3$, and therefore the weight of the smallest error $A_l^\dagger A_k$ that cannot be detected by the code is 3. Finally, we recall that it is a nondegenerate code since the smallest weight for elements of \mathcal{S} (other than identity) is 4, and therefore it is greater than the distance $d = 3$. The encoding for the $[[5,1,3]]$ code is given by [20]

$$|0\rangle \rightarrow |0_L\rangle = \frac{1}{4} \left[|00000\rangle + |11000\rangle + |01100\rangle + |00110\rangle + |00011\rangle + |10001\rangle - |01010\rangle - |00101\rangle + \right. \\ \left. - |10010\rangle - |01001\rangle - |10100\rangle - |11110\rangle - |01111\rangle - |10111\rangle - |11011\rangle - |11101\rangle \right], \quad (9)$$

$$|1\rangle \rightarrow |1_L\rangle = \frac{1}{4} \left[|11111\rangle + |00111\rangle + |10011\rangle + |11001\rangle + |11100\rangle + |01110\rangle - |10101\rangle - |11010\rangle + \right. \\ \left. - |01101\rangle - |10110\rangle - |01011\rangle - |00001\rangle - |10000\rangle - |01000\rangle - |00100\rangle - |00010\rangle \right]. \quad (10)$$

D. Recovery operators

Recall that any error belonging to the Pauli group of n -qubits, $E \in \mathcal{P}_n$, can be written as

$$E = i^\xi \sigma_{k_1}^1 \otimes \cdots \otimes \sigma_{k_n}^n, \quad (11)$$

where $\xi = 0, 1, 2, 3$ and the superscripts on the $\sigma_{k_l}^l$ label the qubits $l = 1, \dots, n$. Furthermore, the subscripts take values $k_l = 0, x, y, z$ (therefore $\sigma_0 \equiv I, \sigma_x \equiv X, \sigma_y \equiv Y, \sigma_z \equiv Z$), and $\sigma_0^l = I^l$ is the identity operator on the l th qubit. Notice that since $\sigma_y^l = -i\sigma_x^l\sigma_z^l$, Eq. (11) can be rewritten as

$$E = i^{\xi'} \sigma_x(a) \sigma_z(b), \quad (12)$$

where $a = a_1 \cdots a_n$ and $b = b_1 \cdots b_n$ are the bit strings of length n , with

$$\sigma_x(a) \equiv (\sigma_x^1)^{a_1} \otimes \cdots \otimes (\sigma_x^n)^{a_n}, \quad (13) \\ \sigma_z(b) \equiv (\sigma_z^1)^{b_1} \otimes \cdots \otimes (\sigma_z^n)^{b_n}.$$

Although the factor $i^{\xi'}$ in Eq. (12) is needed to ensure that \mathcal{P}_n is a group, in many discussions, it is only necessary to work with the quotient group $\mathcal{P}_n / \{\pm I, \pm iI\}$.

There is a one-to-one correspondence between $\mathcal{P}_n / \{\pm I, \pm iI\}$ and the $2n$ -dimensional binary vector space F_2^{2n} whose elements are bit strings of length $2n$ [22]. A vector $v \in F_2^{2n}$ is denoted $v = (a|b)$, where $a = a_1 \cdots a_n$ and $b = b_1 \cdots b_n$ are bit strings of length n . Scalars take values in the Galois field $F_2 = \{0,1\}$, and vector addition adds components modulo 2. In short, $E = i^\xi \sigma_x(a_l) \sigma_z(b_l) \in \mathcal{P}_n \leftrightarrow v_l = (a_l|b_l) \in F_2^{2n}$. For a quantum stabilizer code \mathcal{C} with generators g_1, \dots, g_{n-k} and

$$\mathcal{A}_{\text{corr}} = \{A'_0, A'_1, A'_2, A'_3, A'_4, A'_5, A'_6, A'_7, A'_8, A'_9, A'_{10}, A'_{11}, A'_{12}, A'_{13}, A'_{14}, A'_{15}\} \subseteq \mathcal{A}, \quad (19)$$

where the cardinality of \mathcal{A} defining the channel in Eq. (6) equals 2^{10} . All weight-0 and -1 error operators satisfy the error-correction conditions [21,24]

$$\langle i_L | A_l'^{\dagger} A_m' | j_L \rangle = \alpha_{lm} \delta_{ij} \quad (20)$$

for $l, m \in \{0, 1, \dots, 15\}$ and $i, j \in \{0, 1\}$, with $\langle i_L | j_L \rangle = \delta_{ij}$. The two 16-dimensional orthogonal subspaces \mathcal{V}^{0_L} and \mathcal{V}^{1_L} of \mathcal{H}_2^5 generated by the action of $\mathcal{A}_{\text{corr}}$ on $|0_L\rangle$ and $|1_L\rangle$ are given by

$$\mathcal{V}^{0_L} = \text{Span} \left\{ |v_k^{0_L}\rangle = \frac{A'_k}{\sqrt{p_k}} |0_L\rangle, \right\}, \quad (21)$$

parity check matrix H , the error syndrome $S(E)$ for an error $E \in \mathcal{P}_n \leftrightarrow v_E = (a_E|b_E) \in F_2^{2n}$ is given by the bit string

$$S(E) = H v_E = l_1 \cdots l_{n-k}, \quad (14)$$

where

$$l_j = H^T(j) \cdot v_E = \langle v_j, E \rangle, \quad (15)$$

with $v_j = (a_j|b_j)$ being the image of the generators g_j and $\langle \cdot, \cdot \rangle$ being the symbol for the symplectic inner product [22]. Furthermore, recall that errors with nonvanishing error syndrome are detectable and that a set of invertible error operators $\mathcal{A}_{\text{corr}}$ is correctable if the set given by $\mathcal{A}_{\text{corr}}^\dagger \mathcal{A}_{\text{corr}}$ is detectable [23]. It is straightforward, though tedious, to check that (see Appendix A)

$$S(A_l'^{\dagger} A'_k) \neq 0, \quad \text{with } l, k \in \{0, 1, \dots, 15\}, \quad (16)$$

where $S(A'_k)$ is the error syndrome of the error operator A'_k , defined as

$$S(A'_k) := H^{[[5,1,3]]} v_{A'_k}. \quad (17)$$

The quantity $H^{[[5,1,3]]}$ is the check matrix for the five-qubit code [21],

$$H^{[[5,1,3]]} := \left(\begin{array}{cccc|cccc} 1 & 1 & 0 & 0 & 0 & 0 & 1 & 0 & 1 \\ 0 & 1 & 1 & 0 & 0 & 1 & 0 & 0 & 1 & 0 \\ 0 & 0 & 1 & 1 & 0 & 0 & 1 & 0 & 0 & 1 \\ 0 & 0 & 0 & 1 & 1 & 1 & 0 & 1 & 0 & 0 \end{array} \right), \quad (18)$$

and $v_{A'_k}$ is the vector in the 10-dimensional binary vector space F_2^{10} corresponding to the error operator A'_k . The set of correctable error operators is given by

with $k = 0, 1, \dots, 15$, and

$$\mathcal{V}^{1_L} = \text{Span} \left\{ |v_k^{1_L}\rangle = \frac{A'_k}{\sqrt{p_k}} |1_L\rangle, \right\}, \quad (22)$$

respectively. Notice that $\langle v_l^{i_L} | v_{l'}^{j_L} \rangle = \delta_{ll'} \delta_{ij}$ with $l, l' \in \{0, 1, \dots, 15\}$ and $i, j \in \{0, 1\}$. Therefore it follows that $\mathcal{V}^{0_L} \oplus \mathcal{V}^{1_L} = \mathcal{H}_2^5$. The recovery superoperator $\mathcal{R} \leftrightarrow \{R_l\}$ with $l = 1, \dots, 16$ is defined as [2]

$$R_l := V_l \sum_{i=0}^1 |v_i^{i_L}\rangle \langle v_i^{i_L}|, \quad (23)$$

where the unitary operator V_l is such that $V_l|v_l^{iL}\rangle = |i_L\rangle$ for $i \in \{0,1\}$. Notice that (see Appendix A for the explicit expressions of recovery operators)

$$R_l := V_l \sum_{i=0}^1 |v_l^{iL}\rangle \langle v_l^{iL}| = |0_L\rangle \langle v_l^{0L}| + |1_L\rangle \langle v_l^{1L}|. \quad (24)$$

Notice that $\mathcal{R} \leftrightarrow \{R_l\}$ is a trace-preserving quantum operation, $\sum_{l=1}^{16} R_l^\dagger R_l = I_{32 \times 32}$, since $\{|v_l^{iL}\rangle\}$ with $l = 1, \dots, 16$ and $i_L \in \{0,1\}$ is an orthonormal basis for $\mathcal{H}_2^{\otimes 5}$. Finally, the action of this recovery operation \mathcal{R} on the map $\Lambda^{(5)}(\rho)$ in Eq. (6) yields

$$\Lambda_{\text{recover}}^{(5)}(\rho) \equiv (\mathcal{R} \circ \Lambda^{(5)})(\rho) := \sum_{k=0}^{2^{10}-1} \sum_{l=1}^{16} (R_l A'_k) \rho (R_l A'_k)^\dagger. \quad (25)$$

E. Entanglement fidelity

Entanglement fidelity is a useful performance measure of the efficiency of QECCs. It is a quantity that keeps track of how well the state and entanglement of a subsystem of a larger system are stored, without requiring the knowledge of the complete state or dynamics of the larger system. More precisely, the entanglement fidelity is defined for a mixed state $\rho = \sum_i p_i \rho_i = \text{tr}_{\mathcal{H}_R} |\psi\rangle \langle \psi|$ in terms of a purification $|\psi\rangle \in \mathcal{H} \otimes \mathcal{H}_R$ to a reference system \mathcal{H}_R . The purification $|\psi\rangle$ encodes all the information in ρ . Entanglement fidelity is a measure of how well the channel Λ preserves the entanglement of the state \mathcal{H} with its reference system \mathcal{H}_R . The entanglement fidelity is defined as follows [19]:

$$\mathcal{F}(\rho, \Lambda) := \langle \psi | (\Lambda \otimes I_{\mathcal{H}_R})(|\psi\rangle \langle \psi|) | \psi \rangle, \quad (26)$$

where $|\psi\rangle$ is any purification of ρ , $I_{\mathcal{H}_R}$ is the identity map on $\mathcal{M}(\mathcal{H}_R)$, and $\Lambda \otimes I_{\mathcal{H}_R}$ is the evolution operator extended to the space $\mathcal{H} \otimes \mathcal{H}_R$, on which ρ has been purified. If the quantum operation Λ is written in terms of its Kraus error operators $\{A_k\}$ as $\Lambda(\rho) = \sum_k A_k \rho A_k^\dagger$, then it can be shown that [25]

$$\mathcal{F}(\rho, \Lambda) = \sum_k \text{tr}(A_k \rho) \text{tr}(A_k^\dagger \rho) = \sum_k |\text{tr}(\rho A_k)|^2. \quad (27)$$

This expression for the entanglement fidelity is very useful for explicit calculations. Finally, assuming that

$$\begin{aligned} \Lambda : \mathcal{M}(\mathcal{H}) \ni \rho &\longmapsto \Lambda(\rho) = \sum_k A_k \rho A_k^\dagger \\ &\in \mathcal{M}(\mathcal{H}), \quad \dim_{\mathbb{C}} \mathcal{H} = N, \end{aligned} \quad (28)$$

and choosing a purification described by a maximally entangled unit vector $|\psi\rangle \in \mathcal{H} \otimes \mathcal{H}$ for the mixed state $\rho = 1/\dim_{\mathbb{C}} \mathcal{H} I_{\mathcal{H}}$, we obtain

$$\mathcal{F}\left(\frac{1}{N} I_{\mathcal{H}}, \Lambda\right) = \frac{1}{N^2} \sum_k |\text{tr} A_k|^2. \quad (29)$$

The expression in Eq. (29) represents the entanglement fidelity when no error correction is performed on the noisy channel Λ in Eq. (28).

Here we want to describe the action of $\mathcal{R} \circ \Lambda^{(5)}$ in Eq. (25), restricted to the code subspace \mathcal{C} . Note that the recovery operators can be expressed as

$$R_{l+1} = R_l \frac{A'_l}{\sqrt{\tilde{p}_l}} = (|0_L\rangle \langle 0_L| + |1_L\rangle \langle 1_L|) \frac{A'_l}{\sqrt{\tilde{p}_l}}, \quad (30)$$

with $l \in \{0, \dots, 15\}$. Recalling that $A'_l = A_l^{\dagger}$, it turns out that

$$\begin{aligned} \langle i_L | R_{l+1} A'_k | j_L \rangle &= \frac{1}{\sqrt{\tilde{p}_l}} \langle i_L | 0_L \rangle \langle 0_L | A_l^{\dagger} A'_k | j_L \rangle \\ &+ \frac{1}{\sqrt{\tilde{p}_l}} \langle i_L | 1_L \rangle \langle 1_L | A_l^{\dagger} A'_k | j_L \rangle. \end{aligned} \quad (31)$$

We now need to compute the 2×2 matrix representation $[R_l A'_k]_{\mathcal{C}}$ of each $R_l A'_k$ with $l = 0, \dots, 15$ and $k = 0, \dots, 2^{10} - 1$, where

$$[R_{l+1} A'_k]_{\mathcal{C}} := \begin{pmatrix} \langle 0_L | R_{l+1} A'_k | 0_L \rangle & \langle 0_L | R_{l+1} A'_k | 1_L \rangle \\ \langle 1_L | R_{l+1} A'_k | 0_L \rangle & \langle 1_L | R_{l+1} A'_k | 1_L \rangle \end{pmatrix}. \quad (32)$$

For $l, k = 0, \dots, 15$, we note that $[R_{l+1} A'_k]_{\mathcal{C}}$ becomes

$$\begin{aligned} [R_{l+1} A'_k]_{\mathcal{C}} &= \begin{pmatrix} \langle 0_L | A_l^{\dagger} A'_k | 0_L \rangle & 0 \\ 0 & \langle 1_L | A_l^{\dagger} A'_k | 1_L \rangle \end{pmatrix} \\ &= \sqrt{\tilde{p}_l} \delta_{lk} \begin{pmatrix} 1 & 0 \\ 0 & 1 \end{pmatrix}, \end{aligned} \quad (33)$$

while for any pair (l, k) with $l = 0, \dots, 15$ and $k > 15$, it follows that

$$\langle 0_L | R_{l+1} A'_k | 0_L \rangle + \langle 1_L | R_{l+1} A'_k | 1_L \rangle = 0. \quad (34)$$

We conclude that the only matrices $[R_l A'_k]_{\mathcal{C}}$ with nonvanishing trace are given by

$$[R_s A'_{s-1}]_{\mathcal{C}} = \sqrt{\tilde{p}_{s-1}} \begin{pmatrix} 1 & 0 \\ 0 & 1 \end{pmatrix}, \quad (35)$$

with $s = 1, \dots, 16$. Therefore the entanglement fidelity $\mathcal{F}^{[[5,1,3]]}(\mu, p)$, defined as

$$\begin{aligned} \mathcal{F}^{[[5,1,3]]}(\mu, p) &:= \mathcal{F}^{[[5,1,3]]}\left(\frac{1}{2} I_{2 \times 2}, \mathcal{R} \circ \Lambda^{(5)}\right) \\ &= \frac{1}{(2)^2} \sum_{k=0}^{2^{10}-1} \sum_{l=1}^{16} |\text{tr}([R_l A'_k]_{\mathcal{C}})|^2, \end{aligned} \quad (36)$$

results in

$$\begin{aligned} \mathcal{F}^{[[5,1,3]]}(\mu, p) &= \sum_{m=0}^{15} \tilde{p}_m = p_{00}^4 p_0 + 3 [2 p_{00}^3 p_{10} p_0 + 3 p_{00}^2 p_{01} p_{10} p_0]. \end{aligned} \quad (37)$$

Notice that the expression in Eq. (36) represents the entanglement fidelity after the error-correction scheme provided by the five-qubit code is performed on the noisy channel $\Lambda^{(5)}$. The explicit expression for $\mathcal{F}^{[[5,1,3]]}(\mu, p)$ in Eq. (37) appears in Appendix A.

Note that for arbitrary memory parameter μ ,

$$\lim_{p \rightarrow 0} \mathcal{F}^{[[5,1,3]]}(\mu, p) = 1, \quad \lim_{p \rightarrow 1} \mathcal{F}^{[[5,1,3]]}(\mu, p) = 0, \quad (38)$$

and for $\mu = 0$,

$$\mathcal{F}^{[[5,1,3]]}(0, p) = 4p^5 - 15p^4 + 20p^3 - 10p^2 + 1. \quad (39)$$

We recall that in general, the application of a QECC will lower the error probability as long as the probability of error on an unencoded qubit is less than a certain critical value (threshold probability). This threshold probability value depends on the code, and above such critical value, the use of a coding scheme only makes the information corruption worse. Obviously, in order to make effective use of QEC, a physical implementation of a channel with a sufficiently low error probability as well as a code with a sufficiently high threshold are needed. For instance, the three-qubit repetition code improves the transmission accuracy when the probability of a bit flip on each qubit sent through the underlying channel is less than 0.5. For greater error probabilities, the error-correction process is actually more likely to corrupt the data than an unencoded transmission would be. In our analysis, the failure probability is represented by [26]

$$\mathcal{P}(\mu, p) := 1 - \mathcal{F}(\mu, p), \quad (40)$$

and it gives us an upper bound on the probability with which a generic encoded state will end up at a wrong state. Therefore the five-qubit code is effective only if $\mathcal{P}^{[[5,1,3]]}(\mu, p) < p$. The effectiveness parametric region $\mathcal{D}^{[[5,1,3]]}$ for the five-qubit code is

$$\mathcal{D}^{[[5,1,3]]} := \{(\mu, p) \in [0, 1] \times [0, 1] : \mathcal{P}^{[[5,1,3]]}(\mu, p) < p\}. \quad (41)$$

For the five-qubit code applied for the correction of correlated depolarizing errors, it turns out that for increasing values of the memory parameter μ , the maximum values of the errors probabilities p for which the correction scheme is effective decrease. More generally, the threshold curve $\mu_{\text{th}}^{[[5,1,3]]} = \mu_{\text{th}}^{[[5,1,3]]}(p)$ defining the parametric region where QEC is effective is plotted in Fig. 1. Furthermore, we point out that the presence of correlations in symmetric depolarizing errors does not improve the performance of the five-qubit code since $\mathcal{F}^{[[5,1,3]]}(\mu, p) \leq \mathcal{F}^{[[5,1,3]]}(0, p)$ for those (μ, p) pairs belonging to the parametric region $\mathcal{D}^{[[5,1,3]]}$. Finally, the plots of

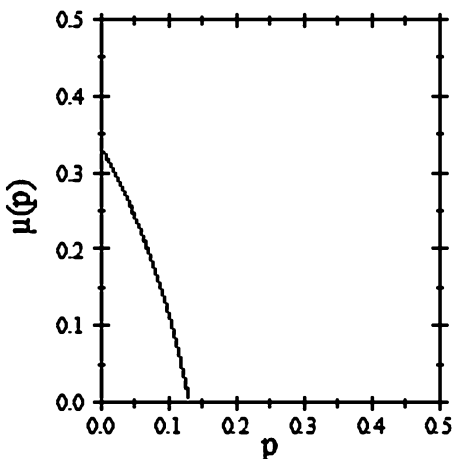


FIG. 1. Threshold curve for the five-qubit code.

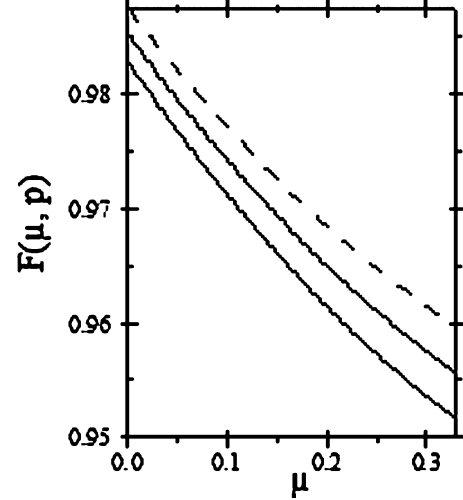


FIG. 2. $\mathcal{F}^{[[5,1,3]]}(\mu, p)$ vs μ with $0 \leq \mu \leq 0.33$ (for $\mu > 0.33$, the error-correction scheme is not effective anymore) for $p = 4.33 \times 10^{-2}$ (thick solid line), $p = 4 \times 10^{-2}$ (thin solid line), and $p = 3.67 \times 10^{-2}$ (dashed line).

$\mathcal{F}^{[[5,1,3]]}(\mu, p)$ versus μ for $p = 4.33 \times 10^{-2}$, $p = 4 \times 10^{-2}$, and $p = 3.67 \times 10^{-2}$ are presented in Fig. 2.

III. THE SEVEN-QUBIT CODE: SYMMETRIC ERROR PROBABILITIES AND CORRELATIONS

In this section, we consider a depolarizing noisy quantum memory channel with symmetric error probabilities, and QEC is performed via the $[[7,1,3]]$ -CSS stabilizer code. The performance of QECCs is quantified by means of the entanglement fidelity $\mathcal{F}^{[[7,1,3]]}(\mu, p)$ as a function of the error probability p and degree of memory μ .

A. Error model

Consider seven qubits and correlated errors in a depolarizing quantum channel $\Lambda^{(7)}(\rho)$:

$$\begin{aligned} \Lambda^{(7)}(\rho) = & \sum_{i_1, i_2, i_3, i_4, i_5, i_6, i_7=0}^3 p_{i_7|i_6} p_{i_6|i_5} p_{i_5|i_4} p_{i_4|i_3} p_{i_3|i_2} p_{i_2|i_1} p_{i_1} \\ & \times [A_{i_7} A_{i_6} A_{i_5} A_{i_4} A_{i_3} A_{i_2} A_{i_1} \rho A_{i_1}^\dagger A_{i_2}^\dagger A_{i_3}^\dagger A_{i_4}^\dagger A_{i_5}^\dagger A_{i_6}^\dagger A_{i_7}^\dagger], \end{aligned} \quad (42)$$

where $A_0 \equiv I$, $A_1 \equiv X$, $A_2 \equiv Y$, $A_3 \equiv Z$ are the Pauli operators and the coefficients $p_{i_l|i_m}$ with $l, m \in \{0, 1, \dots, 7\}$ satisfy the normalization condition

$$\sum_{i_1, i_2, i_3, i_4, i_5, i_6, i_7=0}^3 p_{i_7|i_6} p_{i_6|i_5} p_{i_5|i_4} p_{i_4|i_3} p_{i_3|i_2} p_{i_2|i_1} p_{i_1} = 1. \quad (43)$$

For the depolarizing channel $\Lambda^{(7)}(\rho)$, coefficients $p_{i_l|i_m}$ are explicitly defined in Eq. (5).

B. Error operators

In an explicit way, the depolarizing channel $\Lambda^{(7)}(\rho)$ can be written as

$$\Lambda^{(7)}(\rho) = \sum_{k=0}^{2^{14}-1} A'_k \rho A_k^\dagger, \quad (44)$$

where A'_k are the enlarged error operators acting on the seven-qubit quantum states. The cardinality of the error operators defining $\Lambda^{(7)}(\rho)$ is 2^{14} and is obtained by noticing that

$$\sum_{m=0}^7 3^m \binom{7}{m} = 2^{14}, \quad (45)$$

where $3^m \binom{7}{m}$ is the cardinality of weight- m error operators A'_k in Eq. (44).

C. Encoding

The CSS codes are constructed from two classical binary codes \mathcal{C} and \mathcal{C}' that have the following properties [27,28]: (1) \mathcal{C} and \mathcal{C}' are $[n, k, d]$ and $[n, k', d']$ codes, respectively; (2) $\mathcal{C}' \subset \mathcal{C}$; and (3) \mathcal{C} and \mathcal{C}'_\perp (the dual code of \mathcal{C}') are both t -error correcting codes. For instance, in the case of the seven-qubit code, the two classical codes are the $[7, 4, 3]$ binary Hamming

code (\mathcal{C}) and the $[7, 3, 4]$ binary simplex code (\mathcal{C}'). The dual code \mathcal{C}'_\perp is the $[7, 4, 3]$ binary Hamming code. Thus \mathcal{C} and \mathcal{C}'_\perp are both 1-error correcting codes. In this case, $n = 7$, $k = 4$, $k' = 3$, $k - k' = 1$ so that one qubit is mapped into seven qubits. The seven-qubit code is the simplest example of a CSS code. The five-qubit code introduced in the previous section is the shortest possible quantum code to correct one error and is therefore of immense interest. Although the seven-qubit code is ostensibly more complicated than the five-qubit code, it is actually more useful in certain situations by virtue of being a CSS code. The CSS codes are a particularly interesting class of codes for two reasons. First, they are built using classical codes, which have been more heavily studied than quantum codes, so it is fairly easy to construct useful quantum codes simply by looking at lists of classical codes. Second, because of the form of generators, the CSS codes are precisely those for which a CNOT applied between every pair of corresponding qubits in two blocks performs a valid fault-tolerant operation. This makes them particularly good candidates in fault-tolerant computation.

The $[[7, 1, 3]]$ -CSS code encodes $k = 1$ qubit in $n = 7$ qubits. The cardinality of its stabilizer group \mathcal{S} is $|\mathcal{S}| = 2^{n-k} = 64$, and the set $\mathcal{B}_S^{[[7, 1, 3]]}$ of $n - k = 6$ group generators is given by [21]

$$\mathcal{B}_S^{[[7, 1, 3]]} := \{X^4 X^5 X^6 X^7, X^2 X^3 X^6 X^7, X^1 X^3 X^5 X^7, Z^4 Z^5 Z^6 Z^7, Z^2 Z^3 Z^6 Z^7, Z^1 Z^3 Z^5 Z^7\}. \quad (46)$$

The distance of the code is $d = 3$, and therefore the weight of the smallest error $A_l^\dagger A'_k$ that cannot be detected by the code is 3. Finally, we recall that it is a nondegenerate code since the smallest weight for elements of \mathcal{S} (other than identity) is 4, and therefore it is greater than the distance $d = 3$. The encoding for the $[[7, 1, 3]]$ code is given by [21]

$$|0\rangle \rightarrow |0_L\rangle = \frac{1}{(\sqrt{2})^3} \left[|0000000\rangle + |0110011\rangle + |1010101\rangle + |1100110\rangle + |0001111\rangle + |0111100\rangle + |1011010\rangle + |1101001\rangle \right], \quad (47)$$

$$|1\rangle \rightarrow |1_L\rangle = \frac{1}{(\sqrt{2})^3} \left[|1111111\rangle + |1001100\rangle + |0101010\rangle + |0011001\rangle + |1110000\rangle + |1000011\rangle + |0100101\rangle + |0010110\rangle \right]. \quad (48)$$

D. Recovery operators

Recall that errors with nonvanishing error syndrome are detectable and that a set of invertible error operators $\mathcal{A}_{\text{corr}}$ is correctable if the set given by $\mathcal{A}_{\text{corr}}^\dagger \mathcal{A}_{\text{corr}}$ is detectable [23]. It is straightforward, though tedious, to check that

$$S(A_l^\dagger A'_k) \neq 0, \quad \text{with } l, k \in \{0, 1, \dots, 63\}, \quad (49)$$

where $S(A'_k)$ is the error syndrome of the error operator A'_k (see Appendix B for their explicit expressions), defined as [26]

$$S(A'_k) := H^{[[7, 1, 3]]} v_{A'_k}. \quad (50)$$

The quantity $H^{[[7, 1, 3]]}$ is the check matrix for the seven-qubit code [21]:

$$H^{[[7, 1, 3]]} := \left(\begin{array}{cccccc|cccccc} 1 & 1 & 1 & 1 & 0 & 0 & 0 & 0 & 0 & 0 & 0 & 0 \\ 1 & 1 & 0 & 0 & 1 & 1 & 0 & 0 & 0 & 0 & 0 & 0 \\ 1 & 0 & 1 & 0 & 1 & 0 & 1 & 0 & 0 & 0 & 0 & 0 \\ 0 & 0 & 0 & 0 & 0 & 0 & 0 & 1 & 1 & 1 & 1 & 0 \\ 0 & 0 & 0 & 0 & 0 & 0 & 0 & 1 & 1 & 0 & 0 & 1 \\ 0 & 0 & 0 & 0 & 0 & 0 & 0 & 1 & 0 & 1 & 0 & 1 \end{array} \right), \quad (51)$$

and $v_{A'_k}$ is the vector in the 14-dimensional binary vector space F_2^{14} corresponding to the error operator A'_k . The $[[7, 1, 3]]$ code has distance 3, and therefore all errors $A' \equiv A_l^\dagger A'_k$ with $l, k \in \{0, \dots, 2^{14} - 1\}$ of weight less than 3 satisfy the relation

$$\langle i_L | A' | j_L \rangle = \alpha_{A'} \delta_{ij}, \quad (52)$$

and at least one error of weight 3 exists that violates it. It is straightforward, though tedious, to check that all one- and two-qubit error operators satisfy this equation (therefore they

are detectable). Instead, there are three-qubit errors that do not satisfy Eq. (52). For instance, the error operator $X^1 X^2 X^3$ is such that $\langle 0_L | X^1 X^2 X^3 | 1_L \rangle = 1 \neq 0$. The $[[7,1,3]]$ code corrects arbitrary one-qubit errors, not arbitrary two-qubit errors. In Appendix B, we introduce the Set-1 of correctable errors and explicitly show that they are detectable. It turns out that the set of correctable error operators is given by

$$\mathcal{A}_{\text{corr}} = \{A'_0, A'_1, \dots, A'_{21}, A'_{22}, \dots, A'_{63}\} \subseteq \mathcal{A}, \quad (53)$$

where the cardinality of \mathcal{A} equals 2^{14} . All weight-0, weight-1, and the 42 weight-2 previously mentioned error operators (see Appendix B) satisfy the error-correction conditions

$$\langle i_L | A'_l A'_m | j_L \rangle = \alpha'_{lm} \delta_{ij} \quad (54)$$

for $l, m \in \{0, 1, \dots, 63\}$ and $i, j \in \{0, 1\}$, with $\langle i_L | j_L \rangle = \delta_{ij}$.

In general, QEC protocols are symmetric with respect to the phase and bit bases and so enable the detection and correction of an equal number of phase and bit errors. In the CSS construction, a pair of codes are used, one for correcting the bit-flip errors and the other for correcting the phase-flip errors. These codes can be chosen in such a way that the code correcting the phase-flip errors has a larger distance than the code correcting the bit-flip errors. Therefore the resulting asymmetric quantum code has different error-correcting capability for handling different type of errors. For instance, we emphasize that for the seven-qubit code, there is some freedom in the selection of the set of correctable errors, even after the stabilizer generators have been specified [29]. The seven-qubit code may be designed to prioritize a certain error over others (say, Z errors over X and X errors over Y). For instance, an implementation which has no possibility at all of a Y error could use a code where the set of correctable errors was chosen to exclude corrections for Y . Optimizing the seven-qubit code to completely remove the ability to correct one error could lead to qualitatively different behavior, possibly even including better threshold values [29]. Instead, the five-qubit code (which is not a CSS code) corrects a unique symmetric set of errors. In what follows, first we will compute $\mathcal{F}_{\text{Set-1}}^{[[7,1,3]]}(\mu, p)$, assuming to correct the set of errors in Eq. (53); second, we will compute $\mathcal{F}_{\text{Set-2}}^{[[7,1,3]]}(\mu, p)$, assuming to correct the set of errors where we prioritize Z errors over X and X errors over Y .

E. Computation of $\mathcal{F}_{\text{Set-1}}^{[[7,1,3]]}(\mu, p)$

The two 64-dimensional orthogonal subspaces \mathcal{V}^{0_L} and \mathcal{V}^{1_L} of \mathcal{H}_2^7 generated by the action of $\mathcal{A}_{\text{corr}}$ on $|0_L\rangle$ and $|1_L\rangle$ are given by

$$\mathcal{V}^{0_L} = \text{Span} \left\{ |v_{l+1}^{0_L}\rangle = \frac{1}{\sqrt{\tilde{p}'_l}} A'_l |0_L\rangle \right\}, \quad (55)$$

with $l \in \{0, \dots, 63\}$, and

$$\mathcal{V}^{1_L} = \text{Span} \left\{ |v_{l+1}^{1_L}\rangle = \frac{1}{\sqrt{\tilde{p}'_l}} A'_l |1_L\rangle \right\}, \quad (56)$$

respectively. Notice that $\langle v_{l'}^{i_L} | v_l^{j_L} \rangle = \delta_{ll'} \delta_{ij}$, with $l, l' \in \{0, \dots, 63\}$, and $i, j \in \{0, 1\}$. Therefore it follows that $\mathcal{V}^{0_L} \oplus$

$\mathcal{V}^{1_L} = \mathcal{H}_2^7$. The recovery superoperator $\mathcal{R} \leftrightarrow \{R_l\}$ with $l = 1, \dots, 64$ is defined as [2]

$$R_l := V_l \sum_{i=0}^1 |v_l^{i_L}\rangle \langle v_l^{i_L}|, \quad (57)$$

where the unitary operator V_l is such that $V_l |v_l^{i_L}\rangle = |i_L\rangle$ for $i \in \{0, 1\}$. Notice that

$$R_l := V_l \sum_{i=0}^1 |v_l^{i_L}\rangle \langle v_l^{i_L}| = |0_L\rangle \langle v_l^{0_L}| + |1_L\rangle \langle v_l^{1_L}|. \quad (58)$$

It turns out that the 64 recovery operators are given by

$$R_{l+1} = R_l \frac{A'_l}{\sqrt{\tilde{p}'_l}} = (|0_L\rangle \langle 0_L| + |1_L\rangle \langle 1_L|) \frac{A'_l}{\sqrt{\tilde{p}'_l}}, \quad (59)$$

with $l \in \{0, \dots, 63\}$. Notice that $\mathcal{R} \leftrightarrow \{R_l\}$ is a trace-preserving quantum operation, $\sum_{l=1}^{64} R_l^\dagger R_l = I_{128 \times 128}$, because $\{|v_l^{i_L}\rangle\}$, with $l = 1, \dots, 64$, and $i_L \in \{0, 1\}$ is an orthonormal basis for \mathcal{H}_2^7 . Finally, the action of this recovery operation \mathcal{R} on the map $\Lambda^{(7)}(\rho)$ in Eq. (6) leads to

$$\Lambda_{\text{recover}}^{(7)}(\rho) \equiv (\mathcal{R} \circ \Lambda^{(7)})(\rho) := \sum_{k=0}^{2^{14}-1} \sum_{l=1}^{64} (R_l A'_k) \rho (R_l A'_k)^\dagger. \quad (60)$$

F. Entanglement fidelity

We want to describe the action of $\mathcal{R} \circ \Lambda^{(7)}$ restricted to the code subspace \mathcal{C} . Recalling that $A'_l = A_l^{\dagger \prime}$, it turns out that

$$\begin{aligned} \langle i_L | R_{l+1} A'_k | j_L \rangle &= \frac{1}{\sqrt{\tilde{p}'_l}} \langle i_L | 0_L \rangle \langle 0_L | A_l^\dagger A'_k | j_L \rangle \\ &\quad + \frac{1}{\sqrt{\tilde{p}'_l}} \langle i_L | 1_L \rangle \langle 1_L | A_l^\dagger A'_k | j_L \rangle. \end{aligned} \quad (61)$$

We now need to compute the 2×2 matrix representation $[R_l A'_k]_{\mathcal{C}}$ of each $R_l A'_k$ with $l = 0, \dots, 63$ and $k = 0, \dots, 2^{14} - 1$, where

$$[R_{l+1} A'_k]_{\mathcal{C}} := \begin{pmatrix} \langle 0_L | R_{l+1} A'_k | 0_L \rangle & \langle 0_L | R_{l+1} A'_k | 1_L \rangle \\ \langle 1_L | R_{l+1} A'_k | 0_L \rangle & \langle 1_L | R_{l+1} A'_k | 1_L \rangle \end{pmatrix}. \quad (62)$$

For $l, k = 0, \dots, 63$, we note that $[R_{l+1} A'_k]_{\mathcal{C}}$ becomes

$$\begin{aligned} [R_{l+1} A'_k]_{\mathcal{C}} &= \begin{pmatrix} \langle 0_L | A_l^\dagger A'_k | 0_L \rangle & 0 \\ 0 & \langle 1_L | A_l^\dagger A'_k | 1_L \rangle \end{pmatrix} \\ &= \sqrt{\tilde{p}'_l} \delta_{lk} \begin{pmatrix} 1 & 0 \\ 0 & 1 \end{pmatrix}, \end{aligned} \quad (63)$$

while for any pair (l, k) with $l = 0, \dots, 63$ and $k > 63$, it follows that

$$\langle 0_L | R_{l+1} A'_k | 0_L \rangle + \langle 1_L | R_{l+1} A'_k | 1_L \rangle = 0. \quad (64)$$

We conclude that the only matrices $[R_l A'_k]_{\mathcal{C}}$ with nonvanishing trace are given by $[R_{l+1} A'_l]_{\mathcal{C}}$, with $l = 0, \dots, 63$, where

$$[R_{l+1} A'_l]_{\mathcal{C}} = \sqrt{\tilde{p}'_l} \begin{pmatrix} 1 & 0 \\ 0 & 1 \end{pmatrix}. \quad (65)$$

Therefore the entanglement fidelity $\mathcal{F}_{\text{Set-1}}^{[[7,1,3]]}(\mu, p)$, defined as

$$\begin{aligned} \mathcal{F}_{\text{Set-1}}^{[[7,1,3]]}(\mu, p) &:= \mathcal{F}_{\text{Set-1}}^{[[7,1,3]]} \left(\frac{1}{2} I_{2 \times 2}, \mathcal{R} \circ \Lambda^{(7)} \right) \\ &= \frac{1}{(2)^2} \sum_{k=0}^{2^{14}-1} \sum_{l=1}^{64} |\text{tr}([R_l A'_k]_C)|^2, \end{aligned} \quad (66)$$

becomes [the explicit expression for $\mathcal{F}_{\text{Set-1}}^{[[7,1,3]]}(\mu, p)$ is given in Appendix B]

$$\begin{aligned} \mathcal{F}_{\text{Set-1}}^{[[7,1,3]]}(\mu, p) &= p_{00}^6 p_0 + 6p_{00}^5 p_{10} p_0 + 15p_{00}^4 p_{01} p_{10} p_0 + 6p_{00}^4 p_{10}^2 p_0 \\ &\quad + 24p_{00}^3 p_{01} p_{10}^2 p_0 + 12p_{00}^2 p_{01}^2 p_{10}^2 p_0. \end{aligned} \quad (67)$$

Note that for arbitrary degree of memory μ ,

$$\lim_{p \rightarrow 0} \mathcal{F}_{\text{Set-1}}^{[[7,1,3]]}(\mu, p) = 1, \quad \lim_{p \rightarrow 1} \mathcal{F}_{\text{Set-1}}^{[[7,1,3]]}(\mu, p) = 0, \quad (68)$$

and for vanishing memory parameter $\mu = 0$,

$$\begin{aligned} \mathcal{F}_{\text{Set-1}}^{[[7,1,3]]}(0, p) &= \frac{4}{3} p^7 - \frac{35}{3} p^6 + \frac{112}{3} p^5 - \frac{175}{3} p^4 \\ &\quad + \frac{140}{3} p^3 - \frac{49}{3} p^2 + 1. \end{aligned} \quad (69)$$

We emphasize that the presence of correlations in symmetric depolarizing errors does not improve the performance of the seven-qubit code since $\mathcal{F}_{\text{Set-1}}^{[[7,1,3]]}(\mu, p) \leq \mathcal{F}_{\text{Set-1}}^{[[7,1,3]]}(0, p)$ for those (μ, p) pairs belonging to the parametric region $\mathcal{D}_{\text{Set-1}}^{[[7,1,3]]}$, where the correction scheme is effective:

$$\mathcal{D}_{\text{Set-1}}^{[[7,1,3]]} := \{(\mu, p) \in [0, 1] \times [0, 1] : \mathcal{P}_{\text{Set-1}}^{[[7,1,3]]}(\mu, p) < p\}. \quad (70)$$

Furthermore, it turns out that $\mathcal{F}_{\text{Set-1}}^{[[7,1,3]]}(\mu, p) \leq \mathcal{F}^{[[5,1,3]]}(\mu, p)$ in $\mathcal{D}^{[[5,1,3]]} \cap \mathcal{D}_{\text{Set-1}}^{[[7,1,3]]}$, where the area of the parametric region $\mathcal{D}_{\text{Set-1}}^{[[7,1,3]]}$ is smaller than the area of $\mathcal{D}^{[[7,1,3]]}$ (see Fig. 3). The plots of $\mathcal{F}_{\text{Set-1}}^{[[7,1,3]]}(\mu, p)$ versus μ for $p = 4.33 \times 10^{-2}$,

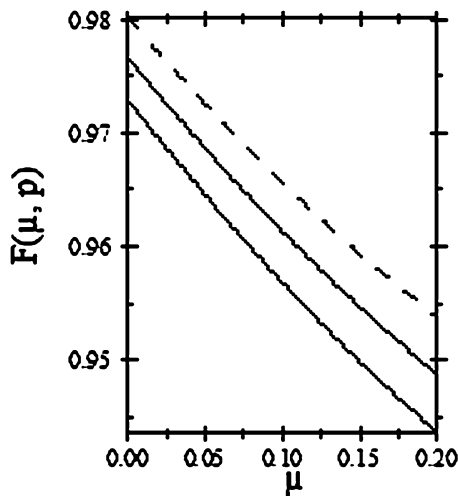


FIG. 3. Symmetric case: Threshold curves $\mu_{\text{th}}^{[[5,1,3]]}(p)$ (dashed line), $\mu_{\text{th,Set-2}}^{[[7,1,3]]}(p)$ (thin solid line), and $\mu_{\text{th,Set-1}}^{[[7,1,3]]}(p)$ (thick solid line) vs p .

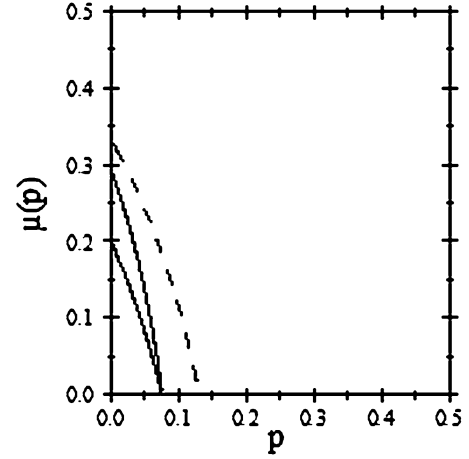


FIG. 4. $\mathcal{F}_{\text{Set-1}}^{[[7,1,3]]}(\mu, p)$ vs μ with $0 \leq \mu \leq 0.199$ (for $\mu > 0.199$, the error-correction scheme is not effective anymore) for $p = 4.33 \times 10^{-2}$ (thick solid line), $p = 4 \times 10^{-2}$ (thin solid line), and $p = 3.67 \times 10^{-2}$ (dashed line).

$p = 4 \times 10^{-2}$, and $p = 3.67 \times 10^{-2}$ appear in Fig. 4. For the seven-qubit code applied for the correction of correlated depolarizing errors in Set-1, it turns out that for increasing values of the memory parameter μ , the maximum values of the error probabilities p for which the correction scheme is effective decrease. For instance, to $\mu_{\text{min}} = 0$ corresponds a threshold $p_{\text{th}} \cong 7.63 \times 10^{-2}$, while to $\mu_{\text{max}} \cong 0.199$ corresponds $p_{\text{th}} \cong 5.04 \times 10^{-4}$.

In the next section, we will study the performance of the seven-qubit code, assuming to correct a new set of correlated error operators. Moreover, we will compare the performance of the code in such two cases and discuss the change of the parametric regions where the quantum correction schemes are effective.

G. Computation of $\mathcal{F}_{\text{Set-2}}^{[[7,1,3]]}(\mu, p)$

Unlike the five-qubit code, the seven-qubit code corrects an asymmetric set of errors. In what follows, we choose the set of correctable errors to prioritize Z errors over X errors over Y errors. Said otherwise, we construct the set of correctable errors by proceeding in increasing order from single-qubit errors to errors of higher weight. Within each level (weight) of errors, we include those that incorporate the most Z errors first. In other words, the sets of weight-0 and weight-1 correctable errors are given in Eqs. (B1) and (B2), respectively. Following the line of reasoning presented in the previous section, after some algebra, it turns out that

$$\begin{aligned} \mathcal{F}_{\text{Set-2}}^{[[7,1,3]]}(\mu, p) &= p_{00}^6 p_0 + 6p_{00}^5 p_{10} p_0 + 15p_{00}^4 p_{01} p_{10} p_0 \\ &\quad + 2p_{00}^4 p_{10} p_0 (p_{11} + 2p_{10}) + 4p_{00}^3 p_{01} p_{10} p_0 \\ &\quad \times (5p_{10} + p_{11}) + 12p_{00}^2 p_{01}^2 p_{10}^2 p_0. \end{aligned} \quad (71)$$

From Eqs. (71) and (67) (see also Appendix B), we obtain

$$\begin{aligned} \mathcal{F}_{\text{Set-2}}^{[[7,1,3]]}(\mu, p) - \mathcal{F}_{\text{Set-1}}^{[[7,1,3]]}(\mu, p) &= (p_{11} - p_{10})(2p_{00}^4 p_{10} p_0 + 4p_{00}^3 p_{01} p_{10} p_0) \geq 0, \end{aligned} \quad (72)$$

with $(p_{11} - p_{10}) = \mu \geq 0$. The explicit expression for $\mathcal{F}_{\text{Set-2}}^{[[7,1,3]]}(\mu, p)$ appears in Appendix B. In the absence of

correlations and considering symmetric error probabilities, the two entanglement fidelities are the same. Therefore we conclude that in the presence of memory effects, it does matter which set of errors we choose to correct, even limiting our analysis to symmetric error probabilities. We will see that the freedom of such choice becomes even more important when combining memory effects and asymmetric error probabilities.

For the seven-qubit code applied for the correction of correlated depolarizing errors in Set-2, it turns out that for increasing values of the memory parameter μ , the maximum values of the error probabilities p for which the correction scheme is effective decrease. For instance, to $\mu_{\min} = 0$ corresponds a threshold $p_{\text{th}} \cong 7.63 \times 10^{-2}$, while to $\mu_{\max} \cong 0.29$ corresponds $p_{\text{th}} \cong 1.95 \times 10^{-3}$.

In conclusion, it follows that in the presence of correlated and symmetric depolarizing errors, the performances of both the five- and seven-qubit quantum codes are lowered. Furthermore, the five-qubit code is characterized by a parametric region (where its correction scheme is effective) that is larger than the one provided by the seven-qubit code (for both selected sets of correctable errors). Furthermore, in the parametric region where both error-correction schemes are effective, the five-qubit code outperforms the seven-qubit code. In the next section, we will discover that the situation is slightly different when considering asymmetries and memory effects in depolarizing channels.

IV. THE FIVE- AND SEVEN-QUBIT CODES: ASYMMETRIC ERROR PROBABILITIES AND CORRELATIONS

In this section, we study the performance of the $[[5,1,3]]$ and $[[7,1,3]]$ QECCs with respect to asymmetric error probabilities ($p = p_X + p_Y + p_Z$ with $p_X \neq p_Y \neq p_Z$) and correlated noise errors in a quantum depolarizing channel.

A. The five-qubit code

In the following discussion, we will assume that the error probability p may be written as

$$p = p_X + p_Y + p_Z, \quad (73)$$

where

$$p_X = \alpha_X p, p_Y = \alpha_Y p, p_Z = \alpha_Z p, \quad (74)$$

with $\alpha_X + \alpha_Y + \alpha_Z = 1$. Notice that in the symmetric case, we simply have $\alpha_X = \alpha_Y = \alpha_Z = 1/3$. Following the line of reasoning presented in Sec. II, it turns out that the $\mathcal{F}_{\text{asym}}^{[[5,1,3]]}(\mu, p)$ becomes

$$\begin{aligned} \mathcal{F}_{\text{asym}}^{[[5,1,3]]}(\mu, p) &= p_{00}^4 p_0 + [p_{00}^3 p_{10} p_0 + 3p_{00}^2 p_{01} p_{10} p_0 + p_{00}^3 p_{01} p_1] \\ &+ [p_{00}^3 p_{20} p_0 + 3p_{00}^2 p_{02} p_{20} p_0 + p_{00}^3 p_{02} p_2] \\ &+ [p_{00}^3 p_{30} p_0 + 3p_{00}^2 p_{03} p_{30} p_0 + p_{00}^3 p_{03} p_3], \end{aligned} \quad (75)$$

where

$$\begin{aligned} p_0 &= 1 - p, \quad p_1 = \alpha_X p, \quad p_2 = \alpha_Y p, \quad p_3 = \alpha_Z p, \\ p_{00} &= (1 - \mu)(1 - p) + \mu, \end{aligned}$$

$$\begin{aligned} p_{01} &= p_{02} = p_{03} = (1 - \mu)(1 - p), \quad p_{10} = \alpha_X p(1 - \mu), \\ p_{20} &= \alpha_Y p(1 - \mu), \quad p_{30} = \alpha_Z p(1 - \mu). \end{aligned} \quad (76)$$

After some straightforward algebra, $\mathcal{F}_{\text{asym}}^{[[5,1,3]]}(\mu, p)$ in Eq. (75) may be written as

$$\begin{aligned} \mathcal{F}_{\text{asym}}^{[[5,1,3]]}(\mu, p) &= p_{00}^4 p_0 + p_{00}^3 p_0 (p_{10} + p_{20} + p_{30}) \\ &+ 3p_{00}^2 p_{01} p_0 (p_{10} + p_{20} + p_{30}) \\ &+ p_{00}^3 p_{01} (p_1 + p_2 + p_3). \end{aligned} \quad (77)$$

Recalling that in the symmetric case, $p_1 = p_2 = p_3 = p/3$, $p_{10} = p_{20} = p_{30} = p/3(1 - \mu)$, and substituting Eq. (76) in Eq. (77), it follows that

$$\mathcal{F}_{\text{asym}}^{[[5,1,3]]}(\mu, p) = \mathcal{F}_{\text{sym}}^{[[5,1,3]]}(\mu, p). \quad (78)$$

Therefore we conclude that the performance of the five-qubit code cannot be enhanced in the case of asymmetric error probabilities in the depolarizing channel. This result was somehow expected since the five-qubit code corrects a unique and symmetric set of error operators.

B. The seven-qubit code

Following the line of reasoning presented in Sec. III, it turns out that the entanglement fidelity $\mathcal{F}_{\text{asym}}^{[[7,1,3]]}(\mu, p)$ evaluated, assuming to correct the Set-2 of error operators, becomes

$$\begin{aligned} \mathcal{F}_{\text{asym}}^{[[7,1,3]]}(\mu, p) &= p_{00}^6 p_0 + 2p_{00}^5 p_{01} (p_1 + p_2 + p_3) \\ &+ 5p_{00}^4 p_{01} p_0 (p_{10} + p_{20} + p_{30}) \\ &+ p_{00}^4 p_0 (2p_{30} p_{33} + p_{30}^2 + 3p_{10} p_{31}) \\ &+ p_{00}^3 p_{01} p_{30} p_0 (8p_{30} + 4p_{33} + 12p_{10}) \\ &+ 6p_{00}^2 p_{01}^2 p_{30} p_0 (p_{30} + p_{10}), \end{aligned} \quad (79)$$

where

$$\begin{aligned} p_0 &= 1 - p, \quad p_1 = \alpha_X p, \quad p_2 = \alpha_Y p, \quad p_3 = \alpha_Z p, \\ p_{00} &= (1 - \mu)(1 - p) + \mu, \\ p_{01} &= p_{02} = p_{03} = (1 - \mu)(1 - p), \quad p_{10} = \alpha_X p(1 - \mu), \\ p_{20} &= \alpha_Y p(1 - \mu), \quad p_{30} = \alpha_Z p(1 - \mu), \\ p_{31} &= p_{30} = \alpha_Z p(1 - \mu), \quad p_{33} = \alpha_Z p(1 - \mu) + \mu. \end{aligned} \quad (80)$$

Notice that for $p_X = p_Y = p_Z = p/3$, $\mathcal{F}_{\text{asym}}^{[[7,1,3]]}(\mu, p)$ equals $\mathcal{F}_{\text{sym}}^{[[7,1,3]]}(\mu, p)$. In the absence of correlations, the entanglement fidelity $\mathcal{F}_{\text{asym}}^{[[7,1,3]]}$ becomes

$$\begin{aligned} \mathcal{F}_{\text{asym}}^{[[7,1,3]]}(0, p) &= (1 - p)^7 + 7p(1 - p)^6 \\ &+ 21p^2(1 - p)^5 [\alpha_Z^2 + \alpha_X \alpha_Z]. \end{aligned} \quad (81)$$

The general expression of $\mathcal{F}_{\text{asym}}^{[[7,1,3]]}(\mu, p)$ is given in Appendix C. We point out that in the absence of correlations, but with asymmetric error probabilities, the seven-qubit code can outperform the five-qubit code:

$$\mathcal{F}_{\text{asym}}^{[[7,1,3]]}(0, p) \geq \mathcal{F}_{\text{asym}}^{[[5,1,3]]}(0, p) \equiv \mathcal{F}_{\text{sym}}^{[[5,1,3]]}(0, p). \quad (82)$$

In Fig. 5, we plot the threshold curves $\mu_{\text{th}}^{[[7,1,3]]}(p)$ and $\mu_{\text{th}}^{[[5,1,3]]}(p)$ versus p in the case case of asymmetric error

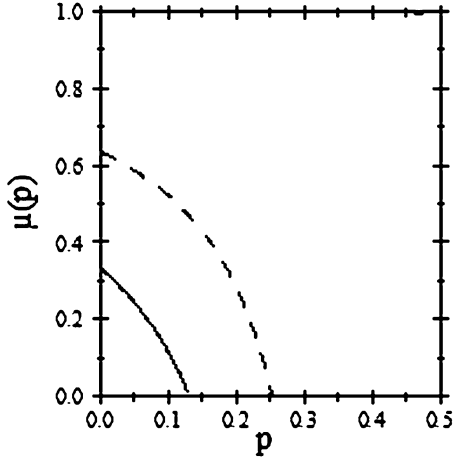


FIG. 5. Asymmetric case: Threshold curves $\mu_{\text{th,Set-2}}^{[[7,1,3]]}(p)$ (dashed line) and $\mu_{\text{th}}^{[[5,1,3]]}(p)$ (thin solid line) vs p .

probabilities. Asymmetries in the error probabilities enlarge the parametric regions where the seven-qubit code is effective for error correction. Furthermore, comparing the performances of such codes in a common region where they are both effective, the seven-qubit code turns out to outperform the five-qubit code in the presence of asymmetries and correlations. In Fig. 6, we plot $\mathcal{F}_{\text{asym}}^{[[7,1,3]]}(\mu, p)$, $\mathcal{F}_{\text{sym}}^{[[5,1,3]]}(\mu, p) = \mathcal{F}_{\text{asym}}^{[[5,1,3]]}(\mu, p)$, and $\mathcal{F}_{\text{sym}}^{[[7,1,3]]}(\mu, p)$ versus the memory parameter μ for $p = 4 \times 10^{-2}$ and $\alpha_Z = 25\alpha$, $\alpha_X = 5\alpha$, and $\alpha_Y = \alpha$, with $\alpha_X + \alpha_Y + \alpha_Z = 1$.

V. FINAL REMARKS

In this article, we have studied the performance of common quantum stabilizer codes in the presence of asymmetric and correlated errors. Specifically, we considered the depolarizing noisy quantum memory channel and performed QEC via the five- and seven-qubit stabilizer codes. We have shown

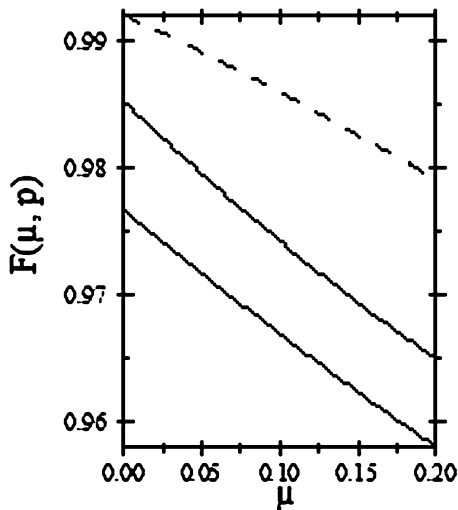


FIG. 6. $\mathcal{F}_{\text{asym}}^{[[7,1,3]]}(\mu, p)$ (dashed line), $\mathcal{F}_{\text{asym}}^{[[5,1,3]]} = \mathcal{F}_{\text{sym}}^{[[5,1,3]]}(\mu, p)$ (thin solid line), and $\mathcal{F}_{\text{sym}}^{[[7,1,3]]}(\mu, p)$ (thick solid line) vs μ with $0 \leq \mu \lesssim 0.199$ (where both error-correction schemes are effective) for $p = 4 \times 10^{-2}$ with $\alpha_Z = 25\alpha$, $\alpha_X = 5\alpha$, and $\alpha_Y = \alpha$.

that memory effects in the error models combined with asymmetries in the error probabilities can produce relevant changes in the performances of QEC schemes by qualitatively affecting the threshold error probability values for which the codes are effective. In summary, we have uncovered the following findings.

1. In the presence of correlated and symmetric depolarizing errors, the performances of both the five- and seven-qubit quantum stabilizer codes are lowered for fixed values of the degree of memory μ . Furthermore, such error-correction schemes only work for low values of μ .

2. In the presence of correlated and symmetric depolarizing errors, the five-qubit code is characterized by a parametric region (where its correction scheme is effective) that is larger than the one provided by the seven-qubit code. Furthermore, in the parametric region where both error-correction schemes are effective, the five-qubit code outperforms the seven-qubit code.

3. The asymmetry in the error probabilities does not affect the performance of the five-qubit code quantified in terms of its entanglement fidelity. On the contrary, it does affect the performance of the seven-qubit code, which is less effective when considering correlated and symmetric depolarizing errors. This peculiar effect is rooted in the stabilizer structure of the CSS seven-qubit code: It is a consequence of the freedom in selecting the set of correctable error operators even after the stabilizer generators have been specified.

4. The performance of the seven-qubit code significantly improves when considering correlated and asymmetric depolarizing errors. Furthermore, in such a case, it is also characterized by higher (than the one provided by the five-qubit code) error probability threshold values. This result confirms that in order to make effective use of QEC, a physical implementation of a channel with a sufficiently low error probability as well as a code with sufficiently high threshold probability is needed [30].

We conclude that in order to optimize the seven-qubit code performance, it is very important to know the experimental details of the physical implementation of the quantum memory channel being considered. Furthermore, in order to make effective use of QEC, a more detailed analysis of the physical noise models for various qubit implementations is needed. This requirement, as we have shown, becomes even more pressing when dealing with noise models in which memory effects are combined with asymmetries in the error probabilities.

ACKNOWLEDGMENTS

C.C. thanks C. Lupo and L. Memarzadeh for useful comments. C.C. is also grateful to V. Aggarwal and R. Calderbank for their kind hospitality and useful discussions during his visit at the Program in Applied and Computational Mathematics at Princeton University. This work was supported by the European Community's Seventh Framework Program under Grant Agreement No. 213681 (CORNER Project No. FP7/2007-2013).

APPENDIX A: THE FIVE-QUBIT CODE

In this appendix, we briefly discuss a few technical details omitted in the article concerning the application of the five-qubit code to the depolarizing memory channel with both symmetric and asymmetric error probabilities.

A. Error operators

The weight-0 and -1 quantum error operators in $\Lambda^{(5)}(\rho)$ in Eq. (6) are given by

$$\begin{aligned}
 A'_0 &= \sqrt{\tilde{p}_0} I^1 \otimes I^2 \otimes I^3 \otimes I^4 \otimes I^5, \\
 A'_1 &= \sqrt{\tilde{p}_1} X^1 \otimes I^2 \otimes I^3 \otimes I^4 \otimes I^5, \\
 A'_2 &= \sqrt{\tilde{p}_2} I^1 \otimes X^2 \otimes I^3 \otimes I^4 \otimes I^5, \\
 A'_3 &= \sqrt{\tilde{p}_3} I^1 \otimes I^2 \otimes X^3 \otimes I^4 \otimes I^5, \\
 A'_4 &= \sqrt{\tilde{p}_4} I^1 \otimes I^2 \otimes I^3 \otimes X^4 \otimes I^5, \\
 A'_5 &= \sqrt{\tilde{p}_5} I^1 \otimes I^2 \otimes I^3 \otimes I^4 \otimes X^5, \\
 A'_6 &= \sqrt{\tilde{p}_6} Y^1 \otimes I^2 \otimes I^3 \otimes I^4 \otimes I^5, \\
 A'_7 &= \sqrt{\tilde{p}_7} I^1 \otimes Y^2 \otimes I^3 \otimes I^4 \otimes I^5, \\
 A'_8 &= \sqrt{\tilde{p}_8} I^1 \otimes I^2 \otimes Y^3 \otimes I^4 \otimes I^5, \\
 A'_9 &= \sqrt{\tilde{p}_9} I^1 \otimes I^2 \otimes I^3 \otimes Y^4 \otimes I^5, \\
 A'_{10} &= \sqrt{\tilde{p}_{10}} I^1 \otimes I^2 \otimes I^3 \otimes I^4 \otimes Y^5, \\
 A'_{11} &= \sqrt{\tilde{p}_{11}} Z^1 \otimes I^2 \otimes I^3 \otimes I^4 \otimes I^5, \\
 A'_{12} &= \sqrt{\tilde{p}_{12}} I^1 \otimes Z^2 \otimes I^3 \otimes I^4 \otimes I^5, \\
 A'_{13} &= \sqrt{\tilde{p}_{13}} I^1 \otimes I^2 \otimes Z^3 \otimes I^4 \otimes I^5, \\
 A'_{14} &= \sqrt{\tilde{p}_{14}} I^1 \otimes I^2 \otimes I^3 \otimes Z^4 \otimes I^5, \\
 A'_{15} &= \sqrt{\tilde{p}_{15}} I^1 \otimes I^2 \otimes I^3 \otimes I^4 \otimes Z^5,
 \end{aligned} \tag{A1}$$

where the coefficients \tilde{p}_l with $l = 0, \dots, 15$ result in

$$\begin{aligned}
 \tilde{p}_0 &= p_{00}^4 p_0, & \tilde{p}_1 &= p_{00}^3 p_{10} p_0, & \tilde{p}_2 &= p_{00}^2 p_{01} p_{10} p_0, \\
 \tilde{p}_3 &= p_{00}^2 p_{01} p_{10} p_0, & \tilde{p}_4 &= p_{00}^2 p_{01} p_{10} p_0, & \tilde{p}_5 &= p_{00}^3 p_{01} p_1, \\
 \tilde{p}_6 &= p_{00}^3 p_{20} p_0, & \tilde{p}_7 &= p_{00}^2 p_{02} p_{20} p_0, & \tilde{p}_8 &= p_{00}^2 p_{02} p_{20} p_0, \\
 \tilde{p}_9 &= p_{00}^2 p_{02} p_{20} p_0, & \tilde{p}_{10} &= p_{00}^3 p_{02} p_2, \\
 \tilde{p}_{11} &= p_{00}^3 p_{30} p_0, & \tilde{p}_{12} &= p_{00}^2 p_{03} p_{30} p_0, & \tilde{p}_{13} &= p_{00}^2 p_{03} p_{30} p_0, \\
 \tilde{p}_{14} &= p_{00}^2 p_{03} p_{30} p_0, & \tilde{p}_{15} &= p_{00}^3 p_{03} p_3,
 \end{aligned} \tag{A2}$$

with

$$\begin{aligned}
 p_0 &= 1 - p, & p_1 &= p_2 = p_3 = \frac{p}{3}, \\
 p_{00} &= (1 - \mu)(1 - p) + \mu, \\
 p_{01} &= p_{02} = p_{03} = (1 - \mu)(1 - p), \\
 p_{10} &= p_{20} = p_{30} = \frac{p}{3}(1 - \mu).
 \end{aligned} \tag{A3}$$

B. Detectable errors

Recall that an error operator A'_k is detectable by the code C if and only if

$$P_C A'_k P_C = \lambda_{A'_k} P_C \tag{A4}$$

for some $\lambda_{A'_k}$, where $P_C := |0_L\rangle\langle 0_L| + |1_L\rangle\langle 1_L|$ is the projector on the code space. On the contrary, a set of error operators $\mathcal{A} = \{A'_i\}$ is correctable if and only if

$$P_C A'_m{}^\dagger A'_n P_C = \lambda_{mn} P_C \tag{A5}$$

for any pair of error operators in \mathcal{A} where λ_{mn} define a positive semidefinite Hermitian matrix. We emphasize that the notion of correctability depends on all the errors in the set under consideration and, unlike detectability, cannot be applied to individual errors. For invertible error operators (such as the ones considered here), there is a simple relationship between detectability and correctability. A set \mathcal{A} is correctable if and only if the operators in the set $\mathcal{A}^\dagger \mathcal{A} := \{A'_1{}^\dagger A'_2 : A'_i \in \mathcal{A}\}$ are detectable. It would be awfully tedious to identify either detectable errors or sets of correctable errors by means of Eqs. (A4) and (A5) for the five- and seven-qubit codes characterized by the code words in Eqs. (9) and (47), respectively. However, the quantum stabilizer formalism allows us to simplify such a task. This is a consequence of the fact that by means of such formalism, it is sufficient to study the effect of the error operators on the generators of the stabilizer and not on the code words themselves. In our work, we have made use of the stabilizer formalism together with the simple relationship between detectability and correctability for invertible error operators in order to identify sets of correctable and detectable errors.

It is known that errors with nonvanishing error syndrome are detectable. It is straightforward to check that

$$S(A'_l{}^\dagger A'_k) \neq 0, \quad \text{with } l, k \in \{0, 1, \dots, 15\}, \tag{A6}$$

where $S(A'_k)$ is the error syndrome of the error operator A'_k , defined as

$$S(A'_k) := H^{[[5,1,3]]} v_{A'_k}. \tag{A7}$$

The quantity $H^{[[5,1,3]]}$ is the check matrix for the five-qubit code in Eq. (18), and $v_{A'_k}$ is the vector in the 10-dimensional binary vector space F_2^{10} corresponding to the error operator A'_k . For instance, considering $k \in \{0, 1, \dots, 15\}$, we obtain

$$\begin{aligned}
 v_I &= (00000|00000), & v_{X^1} &= (10000|00000), \\
 v_{X^2} &= (01000|00000), & v_{X^3} &= (00100|00000), \\
 v_{X^4} &= (00010|00000), & v_{X^5} &= (00001|00000), \\
 v_{Z^1} &= (00000|10000), & v_{Z^2} &= (00000|01000), \\
 v_{Z^3} &= (00000|00100), & v_{Z^4} &= (00000|00010), \\
 v_{Z^5} &= (00000|00001), & v_{Y^1} &= (10000|10000), \\
 v_{Y^2} &= (01000|01000), & v_{Y^3} &= (00100|00100), \\
 v_{Y^4} &= (00010|00010), & v_{Y^5} &= (00001|00001),
 \end{aligned} \tag{A8}$$

and the error syndromes become

$$\begin{aligned}
 S(I) &= 0000, & S(X^1) &= 1000, & S(X^2) &= 1100, \\
 S(X^3) &= 0110, & S(X^4) &= 0011, & S(X^5) &= 0001, \\
 S(Z^1) &= 0101, & S(Z^2) &= 0010, & S(Z^3) &= 1001, \\
 S(Z^4) &= 0100, & S(Z^5) &= 1010, & S(Y^1) &= 1101, \\
 S(Y^2) &= 1110, & S(Y^3) &= 1111, \\
 S(Y^4) &= 0111, & S(Y^5) &= 1011.
 \end{aligned} \tag{A9}$$

For a nondegenerate quantum stabilizer code, linearly independent correctable errors have unequal error syndromes. This necessary (but not sufficient) requirement for a set of correctable errors appears fulfilled in Eq. (A9). Finally, following the previously mentioned line of reasoning, we can show that Eq. (A6) is fulfilled.

C. Recovery operators

From Eq. (24), it follows that the 16 recovery operators are given by

$$\begin{aligned} R_1 &= |0_L\rangle\langle 0_L| + |1_L\rangle\langle 1_L|, & R_2 &= R_1 X^1, & R_3 &= R_1 X^2, \\ R_4 &= R_1 X^3, & R_5 &= R_1 X^4, & R_6 &= R_1 X^5, & R_7 &= R_1 Y^1, \\ R_8 &= R_1 Y^2, & R_9 &= R_1 Y^3, & R_{10} &= R_1 Y^4, \\ R_{11} &= R_1 Y^5, & R_{12} &= R_1 Z^1, & R_{13} &= R_1 Z^2, \\ R_{14} &= R_1 Z^3, & R_{15} &= R_1 Z^4, & R_{16} &= R_1 Z^5. \end{aligned} \quad (\text{A10})$$

D. Entanglement fidelity

The explicit expression for the entanglement fidelity $\mathcal{F}^{[[5,1,3]]}(\mu, p)$ in Eq. (37) is given by

$$\begin{aligned} \mathcal{F}^{[[5,1,3]]}(\mu, p) &= \mu^4(4p^5 - 7p^4 + 3p^3) \\ &\quad + \mu^3(-16p^5 + 36p^4 - 26p^3 + 6p^2) \\ &\quad + \mu^2(24p^5 - 66p^4 + 63p^3 - 24p^2 + 3p) \\ &\quad + \mu(-16p^5 + 52p^4 - 60p^3 + 28p^2 - 4p) \\ &\quad + (4p^5 - 15p^4 + 20p^3 - 10p^2 + 1). \end{aligned} \quad (\text{A11})$$

APPENDIX B: ON THE SEVEN-QUBIT CODE

In this appendix, we briefly discuss a few technical details omitted in the article concerning the application of the seven-qubit code to the depolarizing memory channel with both symmetric and asymmetric error probabilities.

A. Error operators (Set-1)

The set of correctable error operators (Set-1) is explicitly defined by 64 error operators. The only weight-0 error operator is given by

$$A'_0 = \sqrt{\tilde{p}'_0} I^1 \otimes I^2 \otimes I^3 \otimes I^4 \otimes I^5 \otimes I^6 \otimes I^7 \equiv \sqrt{\tilde{p}'_0} I. \quad (\text{B1})$$

The 21 weight-1 error (correctable) operators are given by

$$\begin{aligned} A'_1 &= \sqrt{\tilde{p}'_1} X^1, & A'_2 &= \sqrt{\tilde{p}'_2} X^2, & A'_3 &= \sqrt{\tilde{p}'_3} X^3, \\ A'_4 &= \sqrt{\tilde{p}'_4} X^4, & A'_5 &= \sqrt{\tilde{p}'_5} X^5, & A'_6 &= \sqrt{\tilde{p}'_6} X^6, \\ A'_7 &= \sqrt{\tilde{p}'_7} X^7, & A'_8 &= \sqrt{\tilde{p}'_8} Y^1, & A'_9 &= \sqrt{\tilde{p}'_9} Y^2, \\ A'_{10} &= \sqrt{\tilde{p}'_{10}} Y^3, & A'_{11} &= \sqrt{\tilde{p}'_{11}} Y^4, & A'_{12} &= \sqrt{\tilde{p}'_{12}} Y^5, \\ A'_{13} &= \sqrt{\tilde{p}'_{13}} Y^6, & A'_{14} &= \sqrt{\tilde{p}'_{14}} Y^7, & A'_{15} &= \sqrt{\tilde{p}'_{15}} Z^1, \end{aligned}$$

$$\begin{aligned} A'_{16} &= \sqrt{\tilde{p}'_{16}} Z^2, & A'_{17} &= \sqrt{\tilde{p}'_{17}} Z^3, & A'_{18} &= \sqrt{\tilde{p}'_{18}} Z^4, \\ A'_{19} &= \sqrt{\tilde{p}'_{19}} Z^5, & A'_{20} &= \sqrt{\tilde{p}'_{20}} Z^6, & A'_{21} &= \sqrt{\tilde{p}'_{21}} Z^7. \end{aligned} \quad (\text{B2})$$

Finally, the 42 weight-2 (correctable) error operators are as follows:

$$\begin{aligned} A'_{22} &= \sqrt{\tilde{p}'_{22}} X^1 Z^2, & A'_{23} &= \sqrt{\tilde{p}'_{23}} X^1 Z^3, & A'_{24} &= \sqrt{\tilde{p}'_{24}} X^1 Z^4, \\ A'_{25} &= \sqrt{\tilde{p}'_{25}} X^1 Z^5, & A'_{26} &= \sqrt{\tilde{p}'_{26}} X^1 Z^6, & A'_{27} &= \sqrt{\tilde{p}'_{27}} X^1 Z^7, \\ A'_{28} &= \sqrt{\tilde{p}'_{28}} X^2 Z^1, & A'_{29} &= \sqrt{\tilde{p}'_{29}} X^2 Z^2, & A'_{30} &= \sqrt{\tilde{p}'_{30}} X^2 Z^3, \\ A'_{31} &= \sqrt{\tilde{p}'_{31}} X^2 Z^4, & A'_{32} &= \sqrt{\tilde{p}'_{32}} X^2 Z^5, & A'_{33} &= \sqrt{\tilde{p}'_{33}} X^2 Z^6, \\ A'_{34} &= \sqrt{\tilde{p}'_{34}} X^2 Z^7, & A'_{35} &= \sqrt{\tilde{p}'_{35}} X^3 Z^1, & A'_{36} &= \sqrt{\tilde{p}'_{36}} X^3 Z^2, \\ A'_{37} &= \sqrt{\tilde{p}'_{37}} X^3 Z^3, & A'_{38} &= \sqrt{\tilde{p}'_{38}} X^3 Z^4, & A'_{39} &= \sqrt{\tilde{p}'_{39}} X^3 Z^5, \\ A'_{40} &= \sqrt{\tilde{p}'_{40}} X^3 Z^6, & A'_{41} &= \sqrt{\tilde{p}'_{41}} X^3 Z^7, & A'_{42} &= \sqrt{\tilde{p}'_{42}} X^4 Z^1, \\ A'_{43} &= \sqrt{\tilde{p}'_{43}} X^4 Z^2, & A'_{44} &= \sqrt{\tilde{p}'_{44}} X^4 Z^3, & A'_{45} &= \sqrt{\tilde{p}'_{45}} X^4 Z^4, \\ A'_{46} &= \sqrt{\tilde{p}'_{46}} X^4 Z^5, & & & & \\ A'_{47} &= \sqrt{\tilde{p}'_{47}} X^4 Z^6, & A'_{48} &= \sqrt{\tilde{p}'_{48}} X^4 Z^7, & A'_{49} &= \sqrt{\tilde{p}'_{49}} X^5 Z^1, \\ A'_{50} &= \sqrt{\tilde{p}'_{50}} X^5 Z^2, & A'_{51} &= \sqrt{\tilde{p}'_{51}} X^5 Z^3, & A'_{52} &= \sqrt{\tilde{p}'_{52}} X^5 Z^4, \\ A'_{53} &= \sqrt{\tilde{p}'_{53}} X^5 Z^5, & A'_{54} &= \sqrt{\tilde{p}'_{54}} X^5 Z^6, & A'_{55} &= \sqrt{\tilde{p}'_{55}} X^5 Z^7, \\ A'_{56} &= \sqrt{\tilde{p}'_{56}} X^6 Z^1, & A'_{57} &= \sqrt{\tilde{p}'_{57}} X^6 Z^2, & A'_{58} &= \sqrt{\tilde{p}'_{58}} X^6 Z^3, \\ A'_{59} &= \sqrt{\tilde{p}'_{59}} X^6 Z^4, & A'_{60} &= \sqrt{\tilde{p}'_{60}} X^6 Z^5, & A'_{61} &= \sqrt{\tilde{p}'_{61}} X^6 Z^6, \\ A'_{62} &= \sqrt{\tilde{p}'_{62}} X^6 Z^7, & A'_{63} &= \sqrt{\tilde{p}'_{63}} X^7 Z^1, & & \end{aligned} \quad (\text{B3})$$

B. Detectable errors (Set-1)

For the sake of completeness, we show in an explicit way that these 64 errors are detectable. Considering $k \in \{0, 1, \dots, 21\}$, the error syndrome of weight-0 and weight-1 error operators is given by

$$\begin{aligned} S(I) &= 000000, & S(X^1) &= 111000, & S(X^2) &= 110000, \\ S(X^3) &= 101000, & S(X^4) &= 100000, & S(X^5) &= 011000, \\ S(X^6) &= 010000, & S(X^7) &= 001000, & S(Y^1) &= 111111, \\ S(Y^2) &= 110110, & S(Y^3) &= 101101, & S(Y^4) &= 100100, \\ S(Y^5) &= 011011, & S(Y^6) &= 010010, & S(Y^7) &= 001001, \\ S(Z^1) &= 000111, & S(Z^2) &= 000110, & S(Z^3) &= 000101, \\ S(Z^4) &= 000100, & S(Z^5) &= 000011, \\ S(Z^6) &= 000010, & S(Z^7) &= 000001. \end{aligned} \quad (\text{B5})$$

Instead, for $k \in \{22, \dots, 63\}$, the error syndrome of weight-2 error operators is given by

$$\begin{aligned}
 S(X^1 Z^2) &= 111110, & S(X^1 Z^3) &= 111101, \\
 S(X^1 Z^4) &= 111100, & S(X^1 Z^5) &= 111011, \\
 S(X^1 Z^6) &= 111010, & S(X^1 Z^7) &= 111001, \\
 S(Z^1 X^2) &= 110111, & S(X^2 Z^3) &= 110101, \\
 S(X^2 Z^4) &= 110100, & S(X^2 Z^5) &= 110011, \\
 S(X^2 Z^6) &= 110010, & S(X^2 Z^7) &= 110001, \\
 S(Z^1 X^3) &= 101111, & S(Z^2 X^3) &= 101110, \\
 S(X^3 Z^4) &= 101100, & S(X^3 Z^5) &= 101011, \\
 S(X^3 Z^6) &= 101010, & S(X^3 Z^7) &= 101001, \\
 S(Z^1 X^4) &= 100111, & S(Z^2 X^4) &= 100110, \\
 S(Z^3 X^4) &= 100101, & S(X^4 Z^5) &= 100011, \\
 S(X^4 Z^6) &= 100010, & S(X^4 Z^7) &= 100001, \\
 S(Z^1 X^5) &= 011111, & &
 \end{aligned} \tag{B6}$$

$$\begin{aligned}
 S(Z^2 X^5) &= 011110, & S(Z^3 X^5) &= 011101, \\
 S(Z^4 X^5) &= 011100, & S(X^5 Z^6) &= 011010, \\
 S(X^5 Z^7) &= 011001, & S(Z^1 X^6) &= 010111, \\
 S(Z^2 X^6) &= 010110, & S(Z^3 X^6) &= 010101, \\
 S(Z^4 X^6) &= 010100, & S(Z^5 X^6) &= 010011, \\
 S(X^6 Z^7) &= 010001, & S(Z^1 X^7) &= 001111, \\
 S(Z^2 X^7) &= 001110, & S(Z^3 X^7) &= 001101, \\
 S(Z^4 X^7) &= 001100, & S(Z^5 X^7) &= 001011, \\
 S(Z^6 X^7) &= 001010. & &
 \end{aligned} \tag{B7}$$

Since these errors have nonvanishing error syndromes, they are detectable. As a side remark, we point out that following the previously mentioned line of reasoning, it can be shown that $S(A_l^\dagger A_k') \neq 0$, with $l, k \in \{0, 1, \dots, 63\}$.

C. Entanglement fidelity (Set-1)

The explicit expression for $\mathcal{F}_{\text{Set-1}}^{[[7,1,3]]}(\mu, p)$ in Eq. (67) is given by

$$\begin{aligned}
 \mathcal{F}_{\text{Set-1}}^{[[7,1,3]]}(\mu, p) &= \mu^6 \left(\frac{4}{3} p^7 - p^6 - \frac{5}{3} p^5 + \frac{4}{3} p^4 \right) + \mu^5 \left(-8 p^7 + \frac{50}{3} p^6 - \frac{22}{3} p^5 - 4 p^4 + \frac{8}{3} p^3 \right) + \mu^4 \left(20 p^7 - \frac{205}{3} p^6 \right. \\
 &+ \frac{250}{3} p^5 - 41 p^4 + \frac{14}{3} p^3 + \frac{4}{3} p^2 \left. \right) + \mu^3 \left(-\frac{80}{3} p^7 + \frac{380}{3} p^6 - \frac{680}{3} p^5 + 192 p^4 - \frac{232}{3} p^3 + 12 p^2 \right) \\
 &+ \mu^2 \left(20 p^7 - \frac{365}{3} p^6 + \frac{835}{3} p^5 - 310 p^4 + \frac{530}{3} p^3 - \frac{145}{3} p^2 + 5 p \right) + \mu \left(-8 p^7 + \frac{178}{3} p^6 - \frac{490}{3} p^5 \right. \\
 &+ 220 p^4 - \frac{460}{3} p^3 + \frac{154}{3} p^2 - 6 p \left. \right) + \left(\frac{4}{3} p^7 - \frac{35}{3} p^6 + \frac{112}{3} p^5 - \frac{175}{3} p^4 + \frac{140}{3} p^3 - \frac{49}{3} p^2 + 1 \right). \tag{B8}
 \end{aligned}$$

D. Error operators (Set-2)

The sets of weight-0 and weight-1 correctable errors are given in Eqs. (B1) and (B2), respectively. The chosen set of correctable weight-2 error operators is

$$\begin{aligned}
 A''_{22} &= \sqrt{\tilde{p}''_{22}} Z^1 Z^2, & A''_{23} &= \sqrt{\tilde{p}''_{23}} Z^1 Z^3, & A''_{24} &= \sqrt{\tilde{p}''_{24}} Z^1 Z^4, \\
 A''_{25} &= \sqrt{\tilde{p}''_{25}} Z^1 Z^5, & A''_{26} &= \sqrt{\tilde{p}''_{26}} Z^1 Z^6, & A''_{27} &= \sqrt{\tilde{p}''_{27}} Z^1 Z^7, \\
 A''_{28} &= \sqrt{\tilde{p}''_{28}} Z^2 Z^3, & A''_{29} &= \sqrt{\tilde{p}''_{29}} Z^2 Z^4, & A''_{30} &= \sqrt{\tilde{p}''_{30}} Z^2 Z^5, \\
 A''_{31} &= \sqrt{\tilde{p}''_{31}} Z^2 Z^6, & A''_{32} &= \sqrt{\tilde{p}''_{32}} Z^2 Z^7, & A''_{33} &= \sqrt{\tilde{p}''_{33}} Z^3 Z^4, \\
 A''_{34} &= \sqrt{\tilde{p}''_{34}} Z^3 Z^5, & A''_{35} &= \sqrt{\tilde{p}''_{35}} Z^3 Z^6, & A''_{36} &= \sqrt{\tilde{p}''_{36}} Z^3 Z^7, \\
 A''_{37} &= \sqrt{\tilde{p}''_{37}} Z^4 Z^5, & A''_{38} &= \sqrt{\tilde{p}''_{38}} Z^4 Z^6, & A''_{39} &= \sqrt{\tilde{p}''_{39}} Z^4 Z^7, \\
 A''_{40} &= \sqrt{\tilde{p}''_{40}} Z^5 Z^6, & A''_{41} &= \sqrt{\tilde{p}''_{41}} Z^5 Z^7, & A''_{42} &= \sqrt{\tilde{p}''_{42}} Z^6 Z^7,
 \end{aligned} \tag{B9}$$

$$\begin{aligned}
 A''_{43} &= \sqrt{\tilde{p}''_{43}} Z^1 X^2, & A''_{44} &= \sqrt{\tilde{p}''_{44}} Z^1 X^3, & A''_{45} &= \sqrt{\tilde{p}''_{45}} Z^1 X^4, \\
 A''_{46} &= \sqrt{\tilde{p}''_{46}} Z^1 X^5, & A''_{47} &= \sqrt{\tilde{p}''_{47}} Z^1 X^6, & A''_{48} &= \sqrt{\tilde{p}''_{48}} Z^1 X^7, \\
 A''_{49} &= \sqrt{\tilde{p}''_{49}} Z^2 X^3, & A''_{50} &= \sqrt{\tilde{p}''_{50}} Z^2 X^4, & A''_{51} &= \sqrt{\tilde{p}''_{51}} Z^2 X^5, \\
 A''_{52} &= \sqrt{\tilde{p}''_{52}} Z^2 X^6, & A''_{53} &= \sqrt{\tilde{p}''_{53}} Z^2 X^7, & A''_{54} &= \sqrt{\tilde{p}''_{54}} Z^3 X^4, \\
 A''_{55} &= \sqrt{\tilde{p}''_{55}} Z^3 X^5, & A''_{56} &= \sqrt{\tilde{p}''_{56}} Z^3 X^6, & A''_{57} &= \sqrt{\tilde{p}''_{57}} Z^3 X^7, \\
 A''_{58} &= \sqrt{\tilde{p}''_{58}} Z^4 X^5, & A''_{59} &= \sqrt{\tilde{p}''_{59}} Z^4 X^6, & A''_{60} &= \sqrt{\tilde{p}''_{60}} Z^4 X^7, \\
 A''_{61} &= \sqrt{\tilde{p}''_{61}} Z^5 X^6, & A''_{62} &= \sqrt{\tilde{p}''_{62}} Z^5 X^7, & A''_{63} &= \sqrt{\tilde{p}''_{63}} Z^6 X^7.
 \end{aligned} \tag{B10}$$

E. Entanglement fidelity (Set-2)

The explicit expression for $\mathcal{F}_{\text{Set-2}}^{[[7,1,3]]}(\mu, p)$ in Eq. (71) is given by

$$\begin{aligned}
 \mathcal{F}_{\text{Set-2}}^{[[7,1,3]]}(\mu, p) &= \mu^6 \left(\frac{4}{3} p^7 + p^6 - 5 p^5 + \frac{8}{3} p^4 \right) + \mu^5 \left(-8 p^7 + \frac{20}{3} p^6 + 16 p^5 - \frac{64}{3} p^4 + \frac{20}{3} p^3 \right) \\
 &+ \mu^4 \left(20 p^7 - \frac{145}{3} p^6 + \frac{70}{3} p^5 + 23 p^4 - \frac{70}{3} p^3 + \frac{16}{3} p^2 \right) \\
 &+ \mu^3 \left(-\frac{80}{3} p^7 + \frac{320}{3} p^6 - \frac{460}{3} p^5 + \frac{272}{3} p^4 - \frac{40}{3} p^3 - \frac{16}{3} p^2 + \frac{4}{3} p \right)
 \end{aligned}$$

$$\begin{aligned}
& + \mu^2 \left(20p^7 - \frac{335}{3}p^6 + 235p^5 - \frac{710}{3}p^4 + \frac{350}{3}p^3 - 25p^2 + \frac{5}{3}p \right) \\
& + \mu \left(-8p^7 + \frac{172}{3}p^6 - \frac{460}{3}p^5 + 200p^4 - \frac{400}{3}p^3 + \frac{124}{3}p^2 - 4p \right) \\
& + \left(\frac{4}{3}p^7 - \frac{35}{3}p^6 + \frac{112}{3}p^5 - \frac{175}{3}p^4 + \frac{140}{3}p^3 - \frac{49}{3}p^2 + 1 \right). \tag{B11}
\end{aligned}$$

APPENDIX C: ASYMMETRIES AND CORRELATIONS

A. Entanglement fidelity

Substituting Eq. (80) in Eq. (79), the explicit expression for $\mathcal{F}_{\text{asym}}^{[[7,1,3]]}(\mu, p)$ becomes

$$\begin{aligned}
\mathcal{F}_{\text{asym}}^{[[7,1,3]]}(\mu, p) \\
= \mathcal{A}_6(\mu, p) + \mathcal{A}_5(\mu, p)
\end{aligned}$$

$$\begin{aligned}
& + \mathcal{A}_4(\mu, p) + \mathcal{A}_3(\mu, p) \\
& + \mathcal{A}_2(\mu, p) + \mathcal{A}_1(\mu, p) + \mathcal{A}_0(\mu, p). \tag{C1}
\end{aligned}$$

The quantities $\mathcal{A}_6(\mu, p)$, $\mathcal{A}_5(\mu, p)$, $\mathcal{A}_4(\mu, p)$, and $\mathcal{A}_3(\mu, p)$ are given by

$$\begin{aligned}
\mathcal{A}_6(\mu, p) &= \mu^6 [(6p^7 - 11p^6 + 5p^5) + \alpha_Z(6p^6 - 10p^5 + 4p^4) + (\alpha_Z^2 + \alpha_X\alpha_Z)(-21p^7 + 45p^6 - 30p^5 + 6p^4)], \\
\mathcal{A}_5(\mu, p) &= \mu^5 \left[\begin{aligned} & (-36p^7 + 90p^6 - 74p^5 + 20p^4) + \alpha_Z(-30p^6 + 70p^5 - 52p^4 + 12p^3) \\ & + (\alpha_Z^2 + \alpha_X\alpha_Z)(126p^7 - 330p^6 + 300p^5 - 108p^4 + 12p^3) \end{aligned} \right], \\
\mathcal{A}_4(\mu, p) &= a\mu^4 \left[\begin{aligned} & (90p^7 - 285p^6 + 330p^5 - 165p^4 + 30p^3) + \alpha_Z(60p^6 - 180p^5 + 192p^4 - 84p^3 + 12p^2) \\ & + (\alpha_Z^2 + \alpha_X\alpha_Z)(-315p^7 + 975p^6 - 1110p^5 + 558p^4 - 114p^3 + 6p^2) \end{aligned} \right], \\
\mathcal{A}_3(\mu, p) &= \mu^3 \left[\begin{aligned} & (-120p^7 + 460p^6 - 680p^5 + 480p^4 - 160p^3 + 20p^2) \\ & + \alpha_Z(-60p^6 + 220p^5 - 304p^4 + 192p^3 - 52p^2 + 4p) \\ & + (\alpha_Z^2 + \alpha_X\alpha_Z)(420p^7 - 1500p^6 + 2040p^5 - 1296p^4 + 372p^3 - 36p^2) \end{aligned} \right], \tag{C2}
\end{aligned}$$

while $\mathcal{A}_2(\mu, p)$, $\mathcal{A}_1(\mu, p)$, and $\mathcal{A}_0(\mu, p)$ are

$$\begin{aligned}
\mathcal{A}_2(\mu, p) &= \mu^2 \left[\begin{aligned} & (90p^7 - 405p^6 + 725p^5 - 650p^4 + 300p^3 - 65p^2 + 5p) \\ & + \alpha_Z(30p^6 - 130p^5 + 220p^4 - 180p^3 + 70p^2 - 10p) \\ & + (\alpha_Z^2 + \alpha_X\alpha_Z)(-315p^7 + 1275p^6 - 2010p^5 + 1530p^4 - 555p^3 + 75p^2) \end{aligned} \right], \\
\mathcal{A}_1(\mu, p) &= \mu \left[\begin{aligned} & (-36p^7 + 186p^6 - 390p^5 + 420p^4 - 240p^3 + 66p^2 - 6p) \\ & + \alpha_Z(-6p^6 + 30p^5 - 60p^4 + 60p^3 - 30p^2 + 6p) \\ & + (\alpha_Z^2 + \alpha_X\alpha_Z)(126p^7 - 570p^6 + 1020p^5 - 900p^4 + 390p^3 - 66p^2) \end{aligned} \right], \\
\mathcal{A}_0(\mu, p) &= (1-p)^7 + 7p(1-p)^6 + 21p^2(1-p)^5 [\alpha_Z^2 + \alpha_X\alpha_Z]. \tag{C3}
\end{aligned}$$

- [1] D. Gottesman, e-print [arXiv:0904.2557](https://arxiv.org/abs/0904.2557) [quant-ph] (2009).
[2] E. Knill and R. Laflamme, *Phys. Rev. A* **55**, 900 (1997).
[3] A. R. Calderbank, E. M. Rains, P. W. Shor, and N. J. A. Sloane, *Phys. Rev. Lett.* **78**, 405 (1997).
[4] A. Garg, *Phys. Rev. Lett.* **77**, 964 (1996).
[5] D. Loss and D. P. DiVincenzo, *Phys. Rev. A* **57**, 120 (1998).
[6] W. Y. Hwang, D. D. Ahn, and S. W. Hwang, *Phys. Rev. A* **63**, 022303 (2001).
[7] J. P. Clemens, S. Siddiqui, and J. Gea-Banacloche, *Phys. Rev. A* **69**, 062313 (2004).
[8] R. Klesse and S. Frank, *Phys. Rev. Lett.* **95**, 230503 (2005).
[9] A. Shabani, *Phys. Rev. A* **77**, 022323 (2008).
[10] A. D'Arrigo *et al.*, *Int. J. Quantum. Inf.* **6**, 651 (2008).
[11] C. Cafaro and S. Mancini, *Phys. Lett. A* **374**, 2688 (2010).
[12] O. Astafiev *et al.*, *Phys. Rev. Lett.* **93**, 267007 (2004).
[13] L. Ioffe and M. Mezard, *Phys. Rev. A* **75**, 032345 (2007).
[14] Z. W. E. Evans *et al.*, e-print [arXiv:0709.3875](https://arxiv.org/abs/0709.3875) [quant-ph] (2007).
[15] A. M. Stephens, Z. W. E. Evans, S. J. Devitt, and L. C. L. Hollenberg, *Phys. Rev. A* **77**, 062335 (2008).
[16] P. K. Sarvepalli *et al.*, in IEEE International Symposium on Information Theory, 2008 (unpublished).

- [17] S. A. Aly, e-print [arXiv:0803.0764](https://arxiv.org/abs/0803.0764) [quant-ph] (2008).
- [18] D. Gottesman, Ph.D. thesis, California Institute of Technology, 1997.
- [19] B. Schumacher, *Phys. Rev. A* **54**, 2614 (1996).
- [20] R. Laflamme, C. Miquel, J. P. Paz, and W. H. Zurek, *Phys. Rev. Lett.* **77**, 198 (1996).
- [21] M. A. Nielsen and I. L. Chuang, *Quantum Computation and Information* (Cambridge University Press, Cambridge, 2000).
- [22] R. A. Calderbank *et al.*, *IEEE Trans. Inf. Theory* **44**, 1369 (1998).
- [23] E. Knill *et al.*, e-print [arXiv:quant-ph/0207170](https://arxiv.org/abs/quant-ph/0207170).
- [24] P. Kaye, R. Laflamme, and M. Mosca, *An Introduction to Quantum Computing* (Oxford University Press, Oxford, 2007).
- [25] M. A. Nielsen, e-print [arXiv:quant-ph/9606012](https://arxiv.org/abs/quant-ph/9606012) (1996).
- [26] F. Gaitan, *Quantum Error Correction and Fault Tolerant Quantum Computing* (CRC Press, Boca Raton, 2008).
- [27] A. R. Calderbank and P. W. Shor, *Phys. Rev. A* **54**, 1098 (1996).
- [28] A. M. Steane, *Proc. R. Soc. London, Ser. A* **452**, 2551 (1996).
- [29] D. Zaslavsky, B.S. thesis, Princeton University, 2008.
- [30] E. Knill, *Nature (London)* **434**, 39 (2005).